Advanced Nanocomposites 1 (2024) 120–143

Contents lists available at ScienceDirect

Advanced Nanocomposites

journal homepage: www.keaipublishing.com/en/journals/advanced-nanocomposites/

Nanocomposite design for solid-state lithium metal batteries: Progress, challenge and prospects

Yong Chen[a], Lv Xu[b], Xu Yang[a], Qiongguang Li[c], Meng Yao[b,*], Guoxiu Wang[a,*]

[a] Centre for Clean Energy Technology, School of Mathematical and Physical Sciences, Faculty of Science, University of Technology Sydney, Sydney, NSW 2007, Australia
[b] College of Materials Science and Engineering, Sichuan University, Chengdu 610064, PR China
[c] Anhui Province International Research Center on Advanced Building Materials, School of Materials and Chemical Engineering, Anhui Jianzhu University, Hefei 230601, PR China

ARTICLE INFO

Keywords:
Solid-state lithium metal batteries
Nanocomposite design
Composite polymer electrolytes
Interface compatibility

ABSTRACT

Lithium metal batteries have gained significant attention due to their high energy density, making them a promising candidate for various applications, including electric vehicles and grid-scale energy storage. Nevertheless, the practical development of lithium metal batteries faces challenges related to dendrite formation, low cycling efficiency and poor safety due to the use of liquid electrolytes. Solid-state electrolytes (SSEs) emerge as leading alternatives for next-generation energy storage, offering enhanced safety and superior energy density. However, conventional SSEs fail to meet the simultaneous demands of high ionic conductivity and mechanical resilience, due to their intrinsic solid-state chemical properties. Among the many strategies for enhancing SSE chemistry, composite polymer electrolytes (CPEs) featuring sophisticated nanocomposite designs offer advantageous processability, wettability, superior flexibility, reduced density and cost-effective production. This review thoroughly explores the advantages and roles of advanced nanocomposite designs in CPEs. It delivers crucial insights into the latest advancements in nanocomposite designs for SSEs, guiding future exploration and development initiatives in this vital area.

1. Introduction

The ever-growing demand for electric vehicles and renewable energy has driven the rapid advancement of battery technologies, featuring high energy density and long cycle life [1–3]. Among various battery systems, lithium-ion batteries (LIBs) stand out for their ability to provide energy precisely at the point of demand [4,5]. Since their commercialization in the 1990s, LIBs have been extensively researched and utilized in our daily life [6]. However, current commercial LIBs face challenges in meeting the requirements of energy density, safety, lifespan and cost [7]. Moreover, LIBs are approaching their energy-density limits despite the best available technology today. The increasing demands for grid-scale storage systems and the rapid adoption of electric vehicles have stimulated significant advancements in battery technologies [8]. Consequently, some promising alternatives such as lithium-metal, lithium-sulfur and lithium-air batteries with ultrahigh theoretical energy densities have garnered considerable attention and have been extensively investigated in recent years [8–12].

Nevertheless, the use of metallic Li anodes with traditional liquid electrolytes is often hindered by high safety risks associated with severe Li dendrite growth, which can lead to cell failure and potential fire hazards [13–15]. Furthermore, the commonly used liquid electrolytes in LIBs are not only flammable and prone to leakage, but also exhibit poor thermal stability and have a narrow operating temperature range, thereby posing significant safety hazards [16,17]. Thus, simultaneously realizing high energy density and elevated safety in contemporary LIBs poses a formidable challenge, driving vigorous research into advanced battery systems for the future.

Solid-state electrolytes (SSEs) present a promising solution to fully exploit the high energy density of Li metal, owing to their inherent safety and superior resistance to Li dendrite formation compared to liquid electrolytes [18–23]. SSEs, characterized by excellent mechanical strength, low flammability and leak-proof characteristics, hold great promise for next-generation, high-energy-density lithium metal batteries capable of powering electric vehicles over long distances and enabling smart/multifunctional electronic devices. State-of-the-art SSEs typically fall into three categories, as illustrated in Fig. 1a–c: inorganic solid electrolyte (ISE), solid polymer electrolyte (SPE) and composite polymer electrolyte (CPE) [24]. SPEs, based on polymer-Li salt

Peer review under responsibility of KeAi Communications Co., Ltd.
* Corresponding authors.
E-mail addresses: yaomeng@scu.edu.cn (M. Yao), Guoxiu.Wang@uts.edu.au (G. Wang).

https://doi.org/10.1016/j.adna.2024.03.002
Received 3 February 2024; Received in revised form 6 March 2024; Accepted 15 March 2024
Available online 19 March 2024

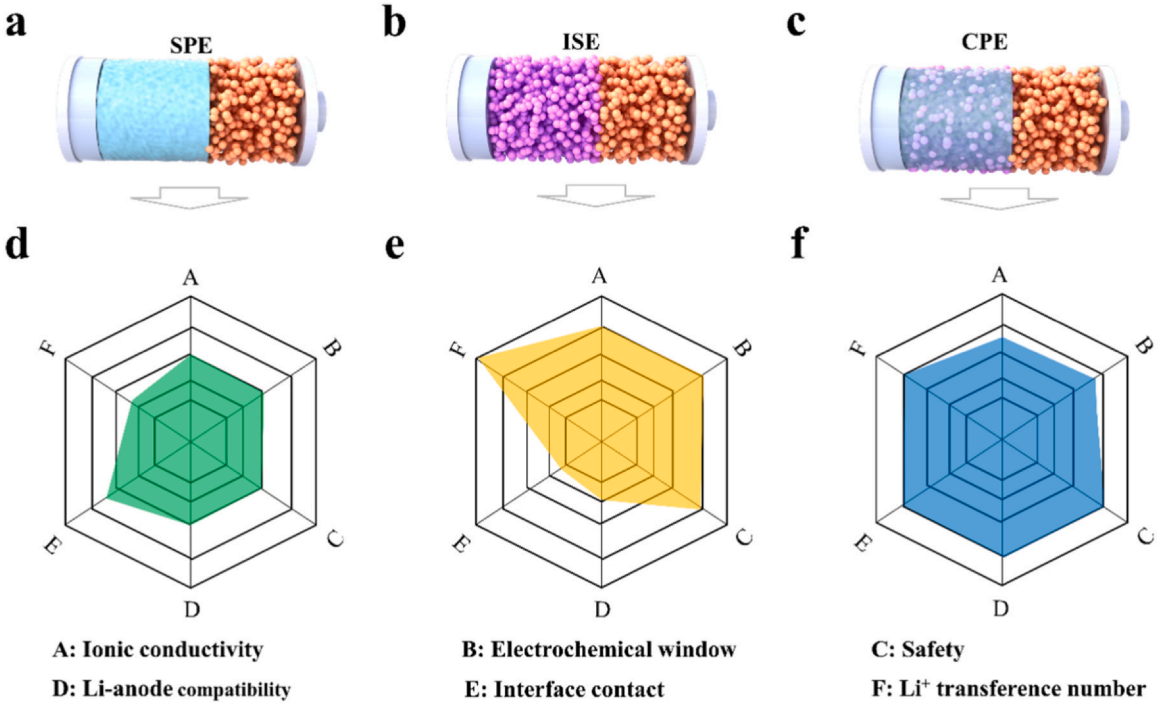

Fig. 1. Important performance comparisons of SPEs a) and d), ISEs b) and e), and CPEs c) and f).

combinations represent a favorable choice as SSEs for fabricating solid-state lithium metal batteries (SSLMBs) because of their processability, wettability, flexibility, low density and cost-effectiveness [20,25]. However, the practical application of SPEs is severely hindered by their limited room temperature (RT) ionic conductivity ($< 10^{-5}$ S cm^{-1}), as shown in Fig. 1d. In contrast, ISEs, particularly sulfides and halides, exhibit promising prospects due to their high RT ionic conductivities (10^{-3}–10^{-2} S cm^{-1}), which are comparable to or even surpassing those of common liquid electrolytes [26–32]. Additionally, ISEs offer advantages such as a high Li^+ transference number (≈ 1) and non-flammability. Nevertheless, the poor interfacial contact performance and high fragility of ISEs significantly impede their practical applications in SSLMBs (see Fig. 1e). Accordingly, CPEs which consist of organic polymers, Li salts and inorganic fillers are currently considered one of the most promising electrolytes meeting industry requirements [22]. CPEs inherit the merits of solid inorganic and organic electrolytes: adequate ionic conductivity, good interfacial contact, appreciable Li^+ transference numbers and importantly, cost-effectiveness and facile synthesis processes (see Fig. 1f).

In a typical CPE system, the commonly used polymer electrolyte hosts include polyethylene oxide (PEO), polymethyl methacrylate (PMMA), polyvinylidene fluoride (PVDF) and its derivatives, and polyacrylonitrile (PAN) (see Fig. 2a) [33–35]. Similar to SPEs, the polymer matrix in a CPE is blended with different lithium salts, such as lithium perchlorate ($LiClO_4$), lithium hexafluorophosphate ($LiPF_6$), lithium bis(trifluoromethyl sulfonyl)imide (LiTFSI), lithium bis(fluor sulfonyl)imide (LiFSI), lithium tetrafluoroborate ($LiBF_4$) and lithium difluoro(oxalate)borate (LiDFOB) [33]. The distinction lies in simultaneously integrating inorganic fillers into polymer-based electrolytes to attain a CPE with high ionic conductivity and improved mechanical properties. Extensive efforts have been devoted to achieving high-performance CPEs, which have significantly contributed to the advancement of battery technology [23,24]. In this regard, the integration of inorganic fillers into the organic polymer matrices to form composite polymer electrolytes has been proven as an effective combination strategy to bridge the gap between SPEs and ISEs [22].

So far, a diverse range of inorganic fillers has been incorporated into polymer-based electrolytes to enhance the performance of the resulting CPEs [8,22]. These inorganic fillers are categorized into two main groups: active and inert fillers, depending on whether they possess ionic conductivity or not, respectively. Active fillers, acting as Li ionic conductors, encompass garnet-type ISEs ($Li_7La_3Zr_2O_{12}$ series, LLZO), perovskite-structured ISEs ($Li_{3x}La_{2/3-x}TiO_3$, LLTO), NASICON (sodium superionic conductor)-type ISEs ($Li_{1+x}Al_xTi_{2x}(PO_4)_3$, LATP and $Li_{1+x}Al_xGe_{2x}(PO_4)_3$, LAGP), which have been extensively investigated (see Fig. 2b) [29]. Meanwhile, inactive fillers include various kinds of oxide ceramics (such as Al_2O_3, SiO_2, ZrO_2, TiO_2), metal-organic-framework materials (MOFs) and boron nitride (BN), etc. [36,37]. A historical timeline depicting the development of CPEs is presented in Fig. 2c, which shows some representative or typical examples [38–53]. Researchers have explored various hybridizations of host components and fillers aiming to achieve high-performance CPEs, emphasizing high ionic conductivity and stable electrochemical performance. However, not all of those strategies have achieved significant effect[22]. Furthermore, numerous hurdles still impede their commercialization [54]. Therefore, the rational design of composite polymer electrolytes is critically important.

Recent studies have revealed the influence of filler structures and their interface chemistry in a polymer/Li salt matrix on Li ionic conducting behavior [36,54]. The size and composition of inorganic fillers in multiphase composites are primary parameters impacting lithium ionic conductivities [55,56]. What's more, the synergetic effect between the organic polymer matrix and inorganic fillers could be "1 + 1 > 2", particularly when employing some advanced nanocomposite strategies to optimize interface design [57–61]. Conclusively, deliberate nanoscale composite design can yield superior comprehensive properties in CPEs, such as good mechanical strength, excellent electrochemical performance and enhanced safety features [62,63]. In this review, we focus on nanocomposite designs within composite polymer electrolytes, with particular emphasis on structural/interfacial design and their possible enhancement mechanisms of electrochemical performances. The interaction between nanofillers and other electrolyte components has been highlighted, in which the ion-conduction mechanisms and interface compatibility are discussed. Then, the nanocomposite strategies are comprehensively outlined and categorized according to the structural and compositional characteristics of fillers in CPEs. Finally, we present the importance and challenges of

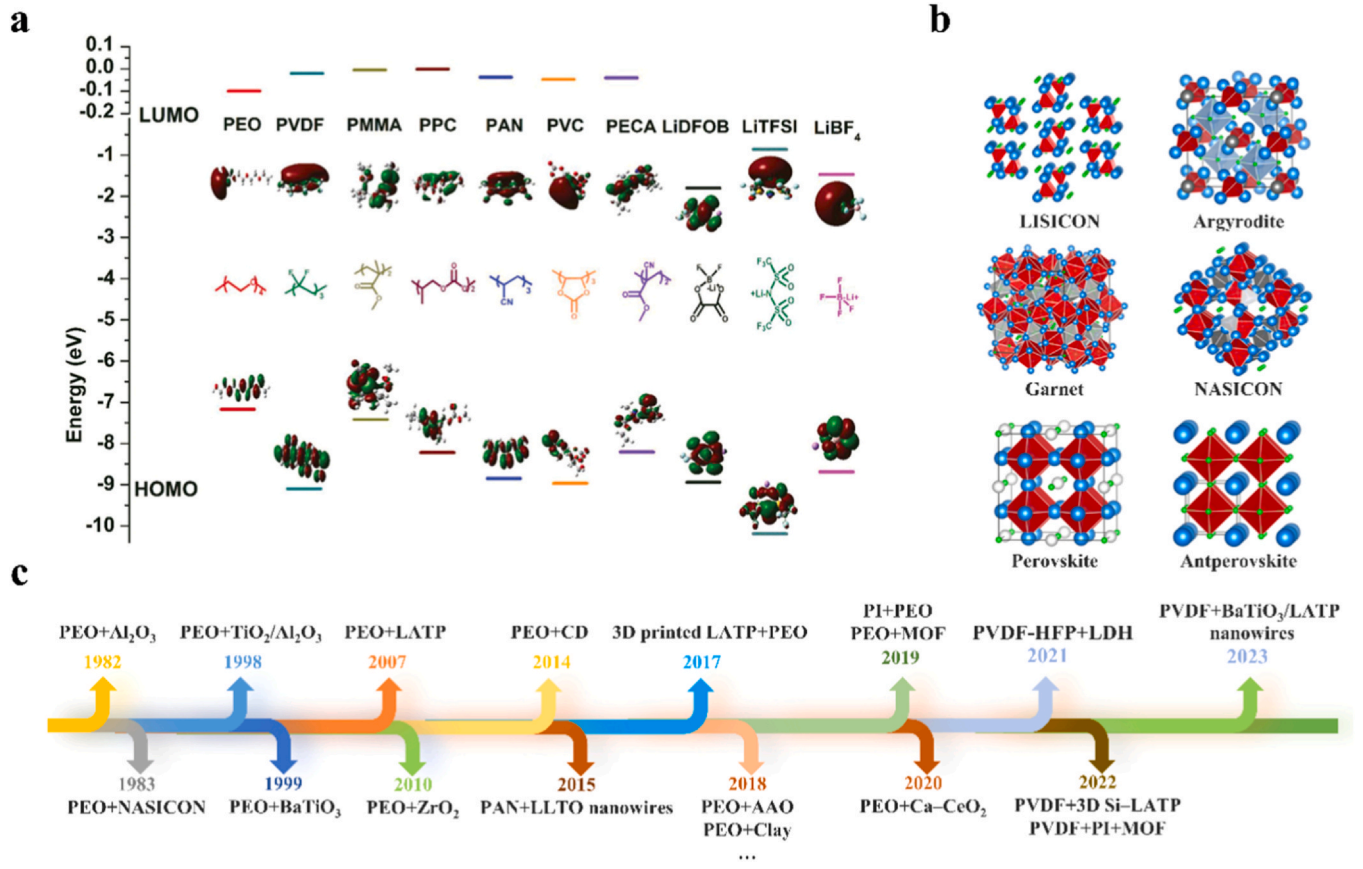

Fig. 2. a) The HOMO and LUMO levels of typical polymer matrices and lithium salts. b) Typical structural families of ISEs (lithium atoms are marked by green spheres). c) A brief historical timeline for the development of the CPEs [38–53].(a) Reproduced with permission [33]. Copyright 2019, Wiley-VCH. (b) Reproduced with permission [29]. Copyright 2022, American Chemical Society.

nanocomposite designs for the practical applications of solid-state lithium metal batteries.

2. General mechanisms of nanocomposite design for high-performance CPEs

Nanocomposite design could be as a highly effective strategy to obtain advanced composite polymer electrolytes (CPEs), enabling substantial improvements in ionic conductivity, Li^+ transference number, electrochemical stability window and mechanical properties. Fundamentally, the elevated ionic conductivity in CPEs can be credited to a synergy of mechanisms: including reducing the crystallinity of polymer matrices, promoting the dissociation of lithium salts, expediting Li^+ transports and introducing ample Li^+ transport channels. Furthermore, through immobilizing or attracting anions within the CPE, enhanced Li^+ transference numbers can be reached [64,65]. Additionally, CPEs incorporate highly thermodynamically and kinetically stable constituents alongside flexible components that exhibit high tensile strength, high elastic modulus and large tensile strain. The nanocomposite design of the CPEs ensures the uniform distribution of these components, bolstering the aforementioned enhancements at the nanoscale.

2.1. Ionic conductivity and transport paths

The properties of polymer chains and filler are the two main factors that affect ion transmission in common CPEs. It is commonly observed that the widely studied PEO-based electrolytes readily form crystalline phases at RT, which leads to limited mobilities of polymer segments and hinders lithium ion transport [35] This is because it is susceptible to crystallization when operating at temperatures close to its glass transition temperature [35]. The utilization of fillers aims primarily to improve the ionic conductivity of polymer-based electrolytes at RT. This hybridization strategy is anticipated to increase the amorphous domains within the polymer matrices and/or facilitate the dissociation of Li salts, which creates more effective ion transport [66]. To date, the properties of various fillers and their effects on the electrochemical properties of CPE have been studied [22]. The generally accepted enhancement mechanism is attributed to the Lewis acid-base effect arising from interactions between the fillers and the polymer-Li salt system, with particular emphasis on the filler-polymer matrix interface [67,68]. Thus, the structural optimization of the interface, involving the size, concentration and dimension of the fillers, represents an effective hybridization strategy for achieving high-performance CPEs.

Three primary types of ionic transmission paths in CPEs can be summarized as follows (Fig. 3a): 1) polymer-chain phase, 2) interfacial phase and 3) percolating active fillers. Increasing interface area has demonstrated a greatly positive correlation with enhanced ion conductivity, attracting considerable attention [45,69–73]. From previous studies, there have been many theories to explain ion transport and its migration paths, including percolation theory, space charge layer theory and effective medium theory [53,74–76]. Due to the complex multiphase structure resulting from polymer-Li salts-filler formations, it is important to understand the ionic enhancement mechanism of CPEs. Despite the reinforcement mechanism is still vague, the goal of fabricating continuous and abundant Li-ion channels remains crucial for achieving fast ion transport. As a result, researchers have explored serials of nanomaterials, including nanoparticles (zero-dimensional material, 0D), nanowires (1D), nanosheets (2D) and three-dimensional nano frameworks (3D), serving as nanofillers in CPEs (Fig. 3b-e) [67,77–79]. Given the widespread and uniformly distrusted phase/phase

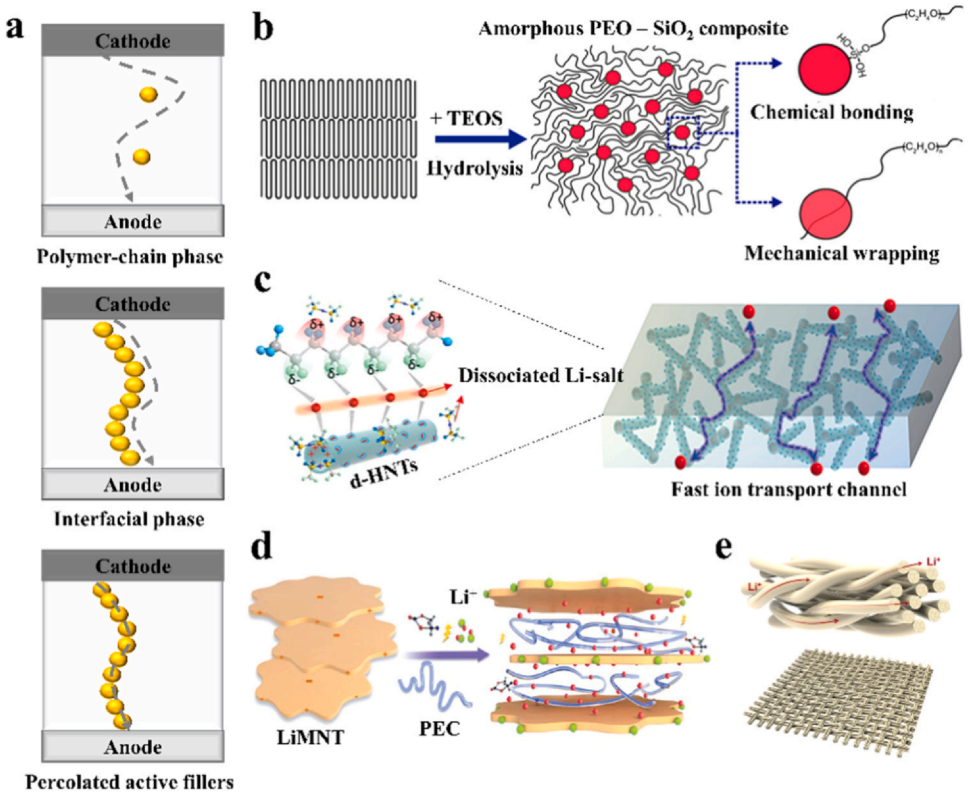

Fig. 3. a) Schematic of different ion transport pathways in CPEs. b) The procedure of in-situ hydrolysis and interaction mechanisms among PEO chains and 0D SiO_2. c) Li^+-transport friendly microenvironment induced by 1D nanomaterials. d) Illustration of the enhancement mechanism of 2D nanomaterials. e) 3D framework.(b) Reproduced with permission [67]. Copyright 2015, American Chemical Society. (c) Reproduced with permission [77]. Copyright 2023, Wiley-VCH. (d) Reproduced with permission [78]. Copyright 2019, Wiley-VCH. (e) Reproduced with permission [79]. Copyright 2018, Elsevier.

interface, the resulting CPEs have superior properties compared to their parent electrolytes.

The Lewis acid-base model of interactions between inorganic fillers and polymer/Li salts is a widely accepted theoretical mechanism for fillers in CPEs [68]. To understand, it is necessary to revisit the ionic transport mechanism in polymer matrices, where the ionic conductivity is dictated by the concentration of mobile lithium ions and their ability to move. As shown in Fig. 4a, polar groups within the organic polymer matrices play a crucial role in facilitating the dissociation of Li salts, resulting in the establishment of a solid-solution system and the consequent generation of mobile lithium ions. However, it is essential to note that the generation mechanism is constrained by the substantial dissociation energy of Li salts within the polymer matrices [80,81]. Significantly, the mobility of Li ions primarily hinges upon the creep of polymer chains and ultimately relies on the crystallinity of the polymer. The inorganic fillers hamper the crystallization of polymer chains surrounding the fillers, augmenting the proportion of amorphous domains. Simultaneously, this enhances the dissociation of Li salts. The enhancement is ascribed to the strong interaction between the fillers and the polar groups in the polymer segments, as well as solvated Li ions or anions [82]. As shown in Fig. 4b, both interactions could contribute to the enhancement of Li-ion transports [54].

Furthermore, the interface plays a vital role in enabling the creation of more mobile Li ions, where a percolation effect was used to interpret the underlying mechanisms [69,83]. Dieterich and co-workers initially proposed the percolation concept for solid-state ionics in 1999 [74], following Armand's pioneering research on SPEs [84]. The interface between a filler and a polymer matrix could establish highly conductive pathways, and many studies have affirmed that interfaces facilitate rapid migration pathways for Li ions [85,86]. Furthermore, space charge layers can be also used to explain interfacial ion transport enhancement. Guo's group identified a "space charge layer" measuring 3 nm in the PEO/LLZO interface. This phenomenon resulted from the redistribution of lithium vacancies and Li ions [76].

2.2. Interfacial compatibility

Interfacial compatibility between SSEs and electrodes has been widely discussed and analyzed. In SSLMBs, the polymer-based electrolytes commonly experience high interfacial resistance at RT, and exhibit limited capacity to suppress lithium dendrites under operating temperatures. They also display inadequate electrochemical stability, especially when paired with high-voltage cathode materials [87–89]. Therefore, improving interfacial compatibility in CPEs focuses on lowering interfacial resistance, enhancing interface stability and boosting Li dendrite suppression.

At a cathode/electrolyte interface, the electrochemical decomposition of polymer/Li salts in SPE is inevitable [87,90–94]. It arises from the inclination toward adopting high-voltage cathode materials to achieve cells with high energy density, while common polymer-based electrolytes are always unstable under high voltages. For example, it is observed that the common PEO-based electrolytes will undergo decomposition when matched with a high-voltage cathode, which is contributed by their oxidation because the PEO chains tend to lose electrons at a high potential [89]. Zhou's group calculated the Highest Occupied Molecular Orbital (HOMO) of the polymer by using the Frontier Molecular Orbital theory to prove the interface instability [95]. It has been widely recognized that PEO-based electrolytes could present an instability beyond the potential of 4.0 V. The terminal hydroxide (–OH) groups in PEO-based electrolytes were also demonstrated to limit their electrochemical stability window, which was compared with poly (ethylene glycol) (PEG) and poly(ethylene glycol)dimethyl ether (PEGDME) with different terminal groups (–OH *vs.* $–OCH_3$, see Fig. 5a) [91].

In addition, the poor solid-solid interfacial contact between SSEs and electrodes would induce a high interfacial resistance, which hinders rate performances and accelerates volume changes in cathode materials during cycling. It is hypothesized that the interaction between fillers and polymer/Li salts can improve the high-voltage compatibility

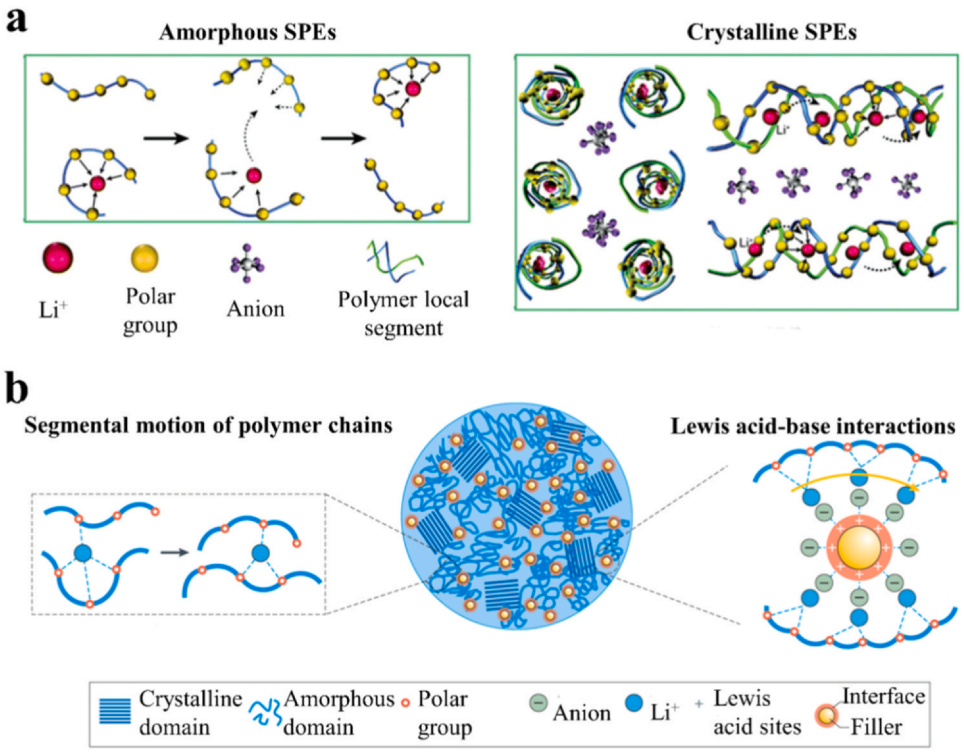

Fig. 4. a) Schematic of ionic conductivity in polymer electrolytes. b) Illustration of ion transport in CPEs.(a) Reproduced with permission [81]. Copyright 2001, Springer Nature. (b) Reproduced with permission [54]. Copyright 2021, Springer Nature.

of CPEs [33,87]. As shown in Fig. 5b, fillers have been proven to enhance the electrochemical stability of CPEs through effective Lewis acid-base interactions, hydrogen-bond interactions, cationic vacancy-salt interactions and ionic dipole-dipole interactions [33]. Recent advancements involved the use of fillers to construct a high-loading composite cathode with 3 wt% carbon-coated LATP nanowires (see Fig. 5c). This innovation enabled an excellent rate performance and cycle stability of SSLBMs with high-mass loadings of up to 15 mg cm^{-2}. The assembled pouch cell demonstrated excellent cycle stability with a high loading of 8.6 mg cm^{-2} (see Fig. 5d) [96].

It should be mentioned that some challenges extend beyond electrolytes to involve the electrode materials. For example, strategies are needed to stabilize the structural stability of nickel-rich cathode and lithium-rich cathode materials [97,98]. Despite utilizing $LiFePO_4$ cathode materials that offer long cycle/calendar life and good safety, various factors can still induce their degradation [99]. Additionally, the oxidation stability of CPEs could also be enhanced effectively by interface modification, including the introduction of stable interface layers and the adjustment of polymer structures and lithium salts [100–107].

At a Li anode/electrolyte interface, pure polymer-based electrolytes cannot suppress Li dendrite formation, which has become a common issue [25]. The incorporation of fillers directly enhances the mechanical strength of CPEs (Fig. 6a) [108]. Furthermore, a large number of studies have shown that fillers could also contribute to increased Li^+ transference numbers, promoting more uniform lithium deposition [54]. For example, Mai's research group introduced spherical core-shell MOFs as nanofillers into the CPE. These spherical nanoparticles are specially designed to improve both ionic conductivity (9.2×10^{-4} S cm^{-1}) and lithium transference number (0.74). As a result, the assembled lithium symmetrical cells displayed outstanding cycle stability against lithium electrodes over 6500 h at RT [109].

In addition, several investigations indicated the formation of favorable artificial interlayers or alloy interfaces prompted by the CPEs [110,111]. For instance, an improved long-term cycling performance in SSLMBs was achieved by the introduction of a single ionic conductor, poly(lithium 4-styrene sulfonate) (PLSS), containing a substantial number of lithium sulfonate groups (-SO_3Li), into Ta-doping garnet ($Li_{6.4}La_3Zr_{1.4}Ta_{0.6}O_{12}$, denoted LLZTO) electrolytes, surpassing the performance of pure LLZTO electrolytes. In a symmetrical lithium battery, this modification exhibited improved cycling performance for 1700 h at 0.2 mA cm^{-2} and 400 h at 0.5 mA cm^{-2} at RT. Li dendrite inhibition was observed by SEM, as shown in Fig. 6b and c [112]. Thus, nanocomposites are beneficial to the uniform distribution of components within the CPEs, inhibiting the formation and growth of lithium dendrites. Moreover, beyond CPEs, inhibiting Li dendrites has involved additional functional modifications, including self-healing materials, dual ion/electron conductive interface layers, dendrite stoppers and the preparation of ultra-high modulus membranes [113–122].

Besides, the advantages of nanocomposites in a CPE can be optimized by some rational membrane preparation technologies. For example, in-situ preparation technology has proven effective in achieving favorable interfacial contacts in SSLMBs [88,123,124]. Recently, He's research group introduced yttria-stabilized zirconia (YSZ) nanoparticles into a poly(1,3-dioxolane) electrolyte prepared using an in-situ technique [125]. It was confirmed that YSZ nanoparticles were acting as Lewis acid fillers due to their propensity to form oxygen vacancies in the YSZ lattice. This kind of oxygen vacancies exhibited an electron-deficiency state, similar to the Zr^{4+} (or Y^{3+}) exposed on the surface of YSZ nanoparticles. This feature made the nanoparticles proficient in adsorbing anion ions and exhibiting Lewis' acidity. Thus, the YSZ nanoparticles functioned not only as catalysts but also as anion adsorbers in the CPEs, resulting in well-dispersed YSZ nanoparticles in the CPE by in-situ preparation. The as-prepared CPE showed a high ionic conductivity of 2.75×10^{-4} S cm^{-1} at RT with an expanded electrochemical window to 4.9 V. Taking advantage of the CPE, those assembled $LiNi_{0.6}Co_{0.2}Mn_{0.2}O_2$/Li batteries exhibited a long cycle life exceeding 800 cycles.

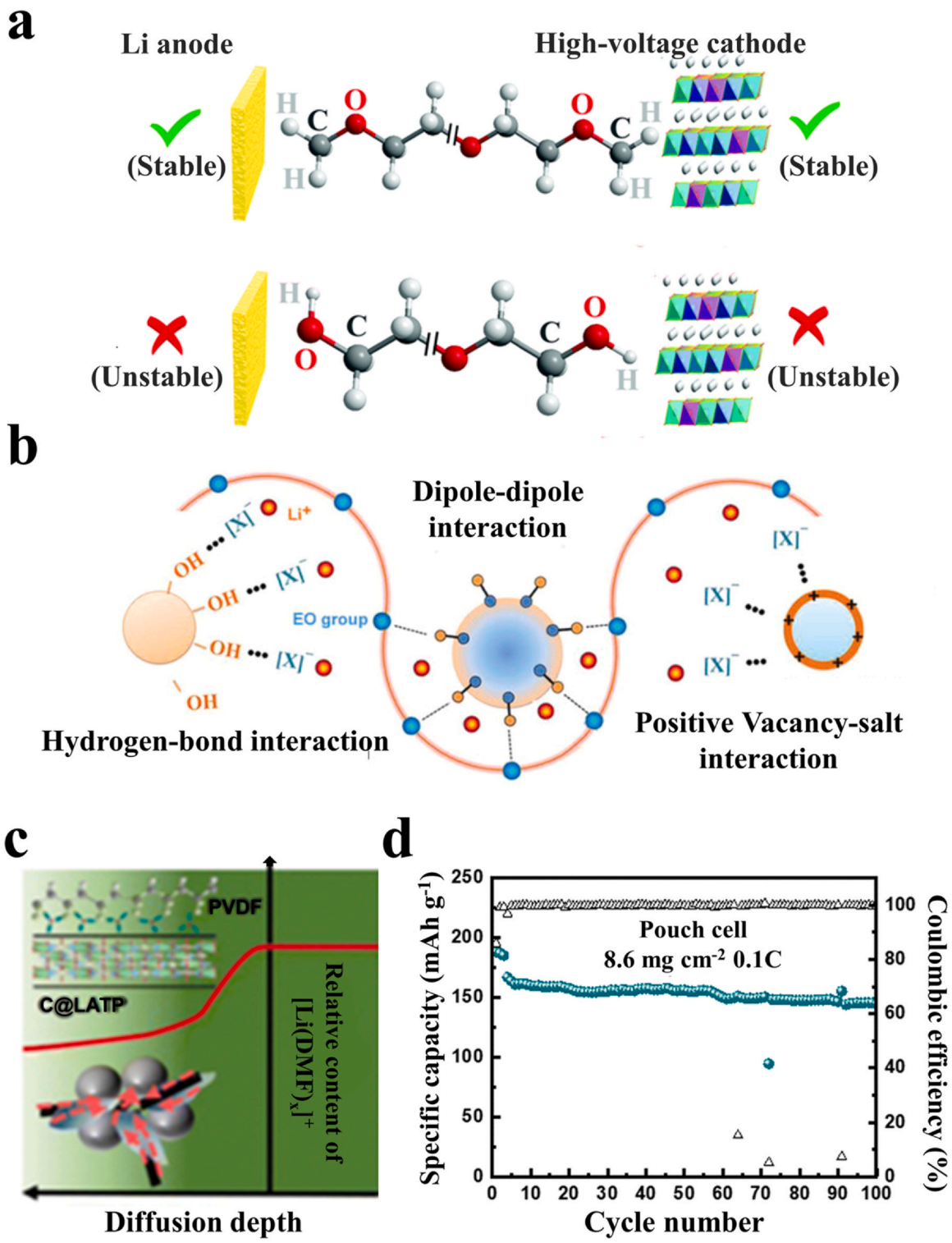

Fig. 5. a) Schematic illustration of PEGDME and PEG response to the Li anode and a high operating voltage. b) Illustration of Lewis acid–base interaction between inorganic additive and polymer electrolyte. c) Schematic of the multiple Li^+ transport channels and diffusion of $[Li(DMF)_x]^+$ in a composite cathode with C@LATP nanowires; and d) the cycling performance of the assembled pouch cell.(a) Reproduced with permission [81]. Copyright 2020, Royal Society of Chemistry. (b) Reproduced with permission [33]. Copyright 2023, Wiley-VCH. (c, d) Reproduced with permission [96]. Copyright 2024, Royal Society of Chemistry.

3. Categories of nanocomposite materials for high-performance CPEs

In contrast to the fillers with a bulk structure, nanocomposite materials feature a high nanoparticle surface area and highly active nanoparticle surface sites. Thus, combining inert or active nanofillers in the composite polymer electrolytes (CPEs) is increasingly recognized as an effective and promising strategy for improving the ionic conductivity, mechanical strength and Li^+ transport number. On the one hand, active nanofillers are anticipated to establish effective pathways for ion transports at the interface between the polymer and the fillers, indicating that the efficiency of ion transport channels varies depending on the dimensions of the nanomaterials used to construct them. On the other hand, surface modification of inert fillers can similarly boost the electrochemical performance of CPEs,

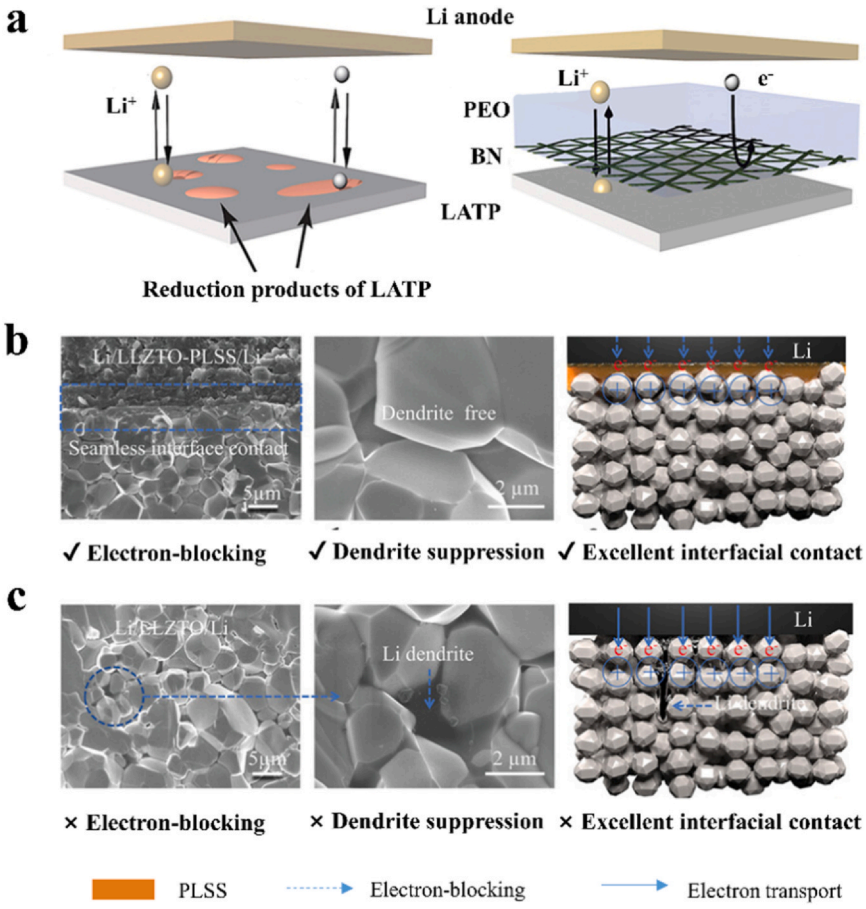

Fig. 6. a) Schematics of the protection mechanism of BN with PEO between a Li anode and LATP. The comparison of cross-sectional SEM image of b) LLZTO-PLSS and c) LLZTO after cycling, as well as schematic illustrations of interface contact of LLZTO-PLSS/Li and LLZTO/Li, respectively.(a) Reproduced with permission [108]. Copyright 2019, Elsevier. (b, c) Reproduced with permission [112]. Copyright 2023, Wiley-VCH.

achieving effects comparable to those of active fillers. Therefore, the dimension is a crucial factor for nanocomposite materials in the design of CPEs, whether they are inert or active fillers. In the subsequent discussion, we will discuss nanofillers based on their respective characteristics. Briefly, the inert and active fillers will be introduced from 0D to 3D respectively, highlighting the importance of nanocomposites.

3.1. Inert fillers

Typical inert fillers mainly include inorganic oxides, such as Al_2O_3, TiO_2 and SiO_2 [54,126–129]. Even though they cannot independently conduct lithium ions, these fillers play a crucial role by providing active sites or regions through physical and/or chemical interactions on their surface. This process hinders the crystallization of polymer chains and promotes the formation of localized amorphous regions associated with the motion capability of polymer segments. Nanocomposite design for CPEs presents superior comprehensive properties compared with the original bulk fillers, so inert fillers with nanocomposite design have become widely studied (Fig. 7) [71,110,130,131]. In terms of dimension, the nanocomposite materials possess a large specific surface area and highly active sites, enabling high performance for CPEs.

3.1.1. 0D inert fillers

Dating back to 1998, Croce et al. first investigated the effect of TiO_2 and Al_2O_3 nanoparticles on PEO electrolytes [40]. The ionic conductivities of as-prepared CPE systems were improved by over three orders of magnitude (to 10^{-5} S cm^{-1} at 30 °C), accompanied by a high Li^+ transference number of 0.6. Further works demonstrated that the surface chemistry of inert fillers produced useful Lewis acid-base interaction [68]. Particulate fillers can readily agglomerate, which could clog ion transporting channels in the CPEs. As a kind of 0D material, quantum dot materials have well-defined sizes generally under 10 nm. It is very suitable to integrate them into the CPEs due to their small size. Recently, Ji et al. proposed graphene quantum dots (GQDs) materials that could be applied to PEO electrolytes [132]. In general, GQDs are composed of single or multi-layer graphene fragments with a diameter of below 10 nm and a thickness of 1–5 nm. There are obvious differences in appearance between PEO/GQD nanocomposite membranes and pure PEO-based electrolyte membranes. Tensile and bending tests have demonstrated that the nanocomposite membranes have shown better mechanical properties than pure PEO-based SPEs. Scanning electron microscope (SEM) studies indicate that the spherulite size is significantly reduced after GQDs are added to polymer electrolytes, indicating that the addition of GQDs affects the crystallinity of PEO and promotes ion dissociation.

In addition to quantum dots, metal/covalent organic framework (MOFs/COFs) materials have garnered significant attention owing to their unique spatial effects that enhance ionic conductivity [133–137]. It is essential to modify the surface of MOF or COF nanomaterials, to obtain lasting and uniform dispersion of 0D nanomaterials. Chen et al. used pentaerythritol tetraacrylate (PETEA) with the dendritic structure to separate Vinyl-ZIF-8 with active functional groups from polyethylene glycol (ethylene glycol) diacrylate (PEGDA). The resulting RT ionic conductivity reaches 6.52×10^{-4} S cm^{-1} [138]. The formation of a three-dimensional cross-linked network tones the mechanical properties of the polymer electrolytes, balancing the mechanical properties (tensile strength 1.85 MPa, elongation at break 45.4 %) and the ionic conductivity (see Fig. 8a). The resulting three-dimensional cross-linked polymer electrolyte not only promotes the rapid movement of Li^+ but also inhibits the growth of lithium dendrites. Certain symmetric Li cells assembled with a CPE derived from MOFs were cycled for 2000 h at a current density of 0.1 mA cm^{-2}.

Besides, researchers are focusing on advancing the functional design of 0D nanomaterials. For instance, Zhu et al. employed PEO as a

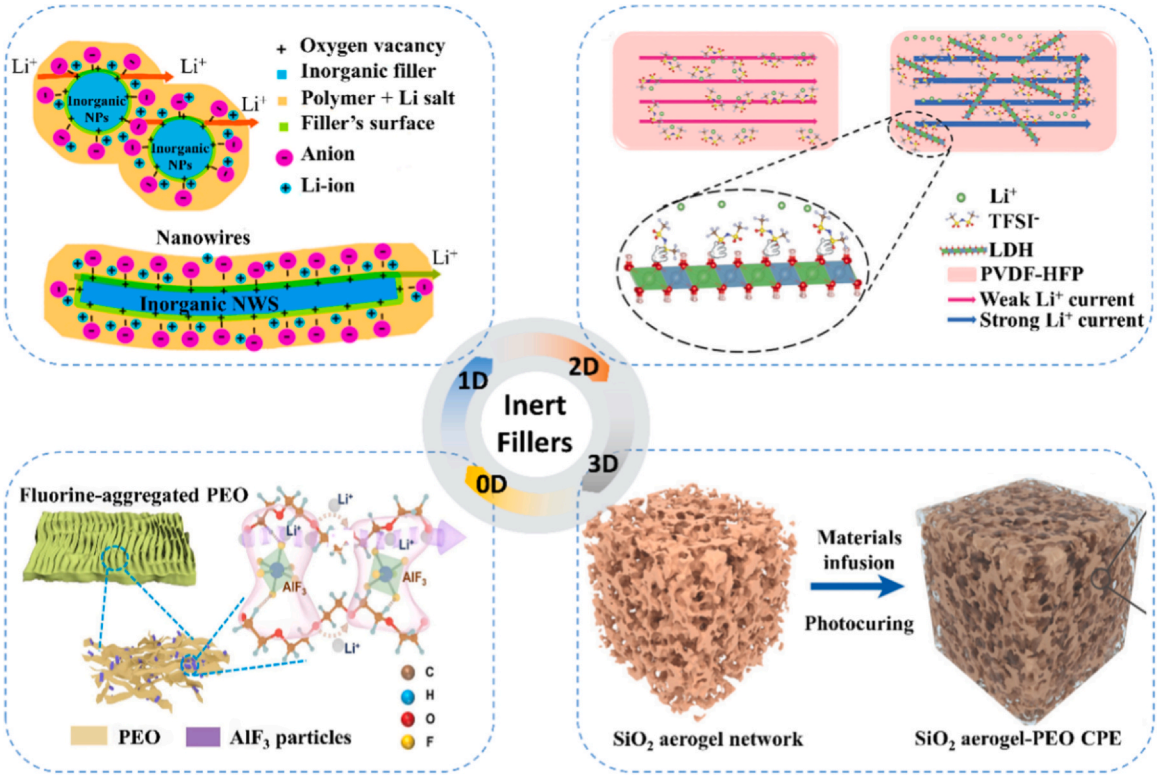

Fig. 7. Demonstration of some inorganic inert fillers, containing 0D, 1D, 2D and 3D components.Reproduced with permission [110]. Copyright 2023, Springer Nature. Reproduced with permission [71]. Copyright 2016, American Chemical Society. Reproduced with permission [130]. Copyright 2021, Wiley-VCH. Reproduced with permission [131]. Copyright 2018, Wiley-VCH.

polymer matrix and incorporated nano indium oxide (nano-In_2O_3) as multifunctional nanofillers to effectively mitigate the undesirable shuttle effect induced by the dissolution of lithium polysulfide (LiPSs) in Li-S batteries [139]. This approach not only significantly enhances the ionic conductivity and mechanical strength of PEO-based electrolytes, but also establishes a compact Li-In alloy layer at the lithium metal anode interface. This Li-In alloy layer further promotes the uniform deposition of Li^+ and suppresses the growth of lithium dendrites. Therefore, the symmetric lithium cell using PEO/LiTFSI/In_2O_3 SPE showed excellent interface stability at a current density of 0.1 mA cm^{-2} with a capacity of 0.1 mAh cm^{-2} (see Fig. 8b). The initial overpotential was only 0.027 V and the cyclic charging and discharging remained stable for over 1200 h in the resulting symmetric Li batteries. The Li-S full cells integrating with PEO/LiTFSI/In_2O_3 CPE exhibited an initial capacity of 695 mAh g^{-1}, and the capacity decay rate after 100 cycles was 0.027 % with a high Coulombic efficiency of nearly 100 %, indicating its highly stable cycling performance. In contrast, the initial capacity of the corresponding PEO/LiTFSI SPE batteries delivered only 394 mAh g^{-1} (see Fig. 8c).

3.1.2. 1D inert fillers

Changing target morphology from 0D to 1D can not only further increase the surface area of the nanofillers, but also help to establish efficient ion transfer pathways. In brief, 1D nanofillers with a high aspect ratio can be beneficial for creating extended and continuous ion channels, in contrast to 0D nanoparticles that offer short and isolated ion transport pathways. Typical 1D materials consist of nanorods, nanotubes, nanowires, small widths of nanosheets, etc. Similar to 0D nanomaterials, the surface charge adjustment can further strengthen the interaction between the nanofillers and the polymer-based electrolytes. Recently, Lv et al. proposed surface-charged halloysite nanotubes (D-HNTs) as dopants for PVDF-based electrolytes to form a nano-dipole-doped composite polymer electrolyte (NDCPE). The resulting NDCPE with only 5 wt% D-HNTs exhibited a high Li^+ transference numbers (0.75 ± 0.04) and a robust dynamic Li^+ interface for achieving high mechanical strength and separator-like toughness, benefiting from the electrostatic interaction between ions and D-HNTs (see Fig. 8d) [77]. The NDCPE battery delivered an initial capacity of 148 mAh g^{-1} and a capacity retention rate of 80 % after 300 cycles, much higher than original PVDF-based SPE batteries (142 mAh g^{-1}, 35 %).

It is feasible to construct a heterostructure in 1D nanomaterials, realizing the functionalization of nanomaterials in space. Deng et al. introduced a novel one-dimensional ferroelectric ceramic-based $Bi_4Ti_3O_{12}$-BiOBr heterojunction nanofiber (BIT-BOB HNFs) into the PEO matrix to construct a lithium-ion conduction highway with “dissociator” and “acceleration zones” [140]. As a 1D ceramic filler, BIT-BOB HNFs could not only construct long-distance organic/inorganic interfaces as ion transport channels but also supply "dissociator" and "accelerating zones" in these channels by adding an electric dipole layer employing its built-in electric field, promoting the dissociation of lithium salts and the transfer of lithium ions. The mechanical properties of CPEs were greatly improved by the introduction of BIT-BOB HNFs. The lithium-ion conductivity and transfer number were both improved by the usage of BIT-BOB HNFs (6.67×10^{-4} S cm^{-1} and 0.54 at 50 °C, respectively). The assembled lithium-lithium symmetric batteries with the optimized CPEs demonstrated cycle stability of over 4500 h at 50 °C. After the assembly of the $LiFePO_4$/Li full cell, the initial discharge of the resulting cells at 0.2 mA cm^{-2} was as high as 155.5 mAh g^{-1}, and the capacity remained at 135.4 mAh g^{-1} after 2200 cycles at 50 °C. Furthermore, assembling $LiNi_{0.8}Co_{0.1}Mn_{0.1}O_2$/Li batteries with the CPE was found to demonstrate stability over 300 cycles at a high cut-off voltage of 4.3 V with a current density of 0.1 mA cm^{-2}. Thus, spatially functionalizing 1D nanomaterials in the composite phase is a productive approach to enhance functionality.

Moreover, the action sites on the surface of 1D nanomaterials are continuously compared with 0D nanomaterials. Wang et al. obtained optimal ionic conductivity and interfacial stability by embedding 1D-TiO_2 fillers rich in oxygen vacancies controlled by morphology and

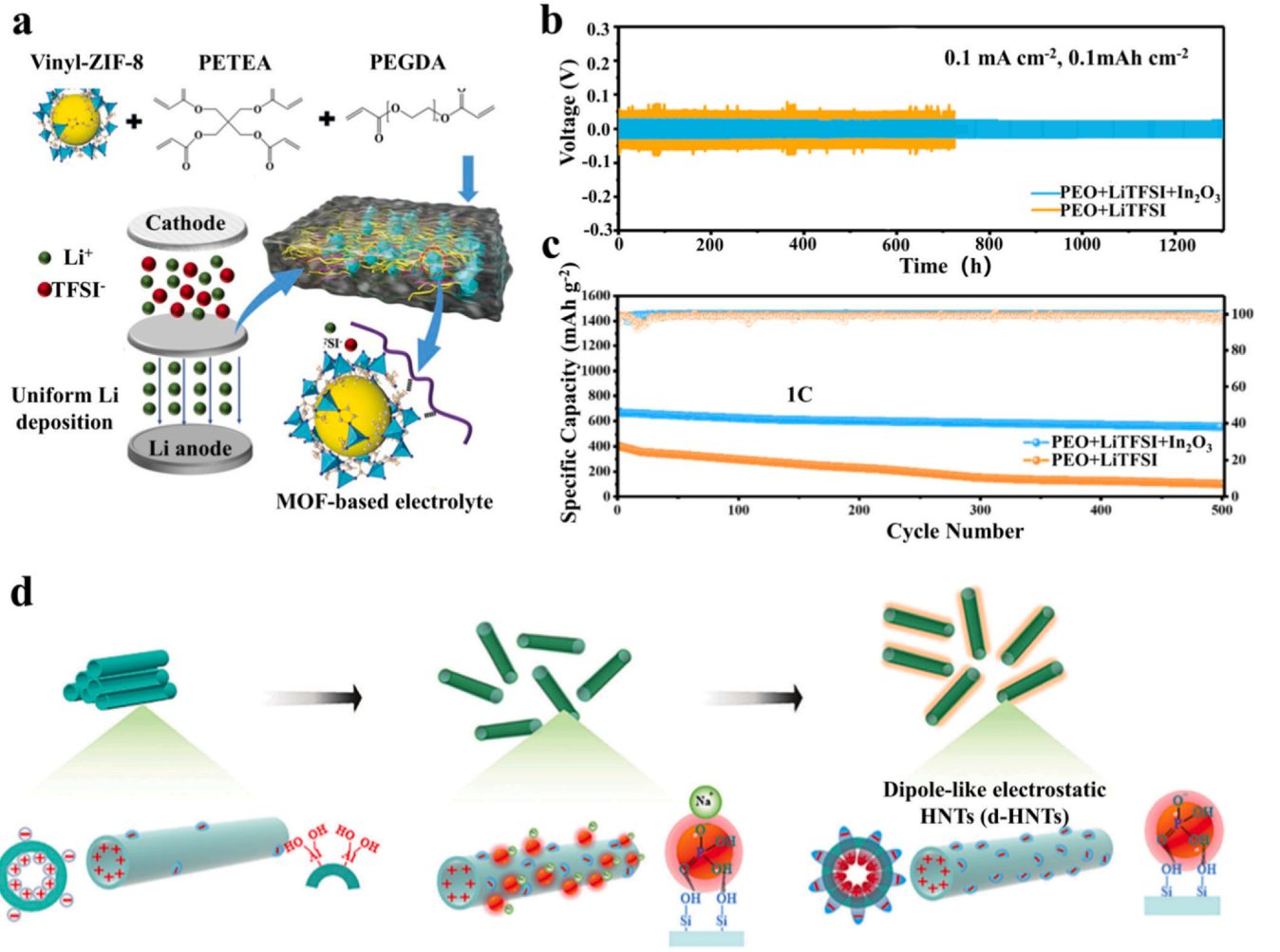

Fig. 8. a) Main chemicals for the synthesis of crosslinked polymers and illustration of conduction for lithium ions. b) Lithium symmetric cell performance cycled at a current density of 0.1 mA cm^{-2} with a capacity of 0.1 mAh cm^{-2}; and c) long cycling performance of solid-state Li-S battery using PEO/LiTFSI/In_2O_3 SPE and PEO/LiTFSI SPE at 60 °C and 1 C [139]. d) Schematic illustration of the preparation of D-HNTs as an advanced nano-dipole doping agent for NDCPE.(a) Reproduced with permission [138]. Copyright 2023, Wiley-VCH. (c) Copyright 2022, Elsevier. (d) Reproduced with permission [77]. Copyright 2023, Wiley-VCH.

defects [141]. 1D-structured TiO_2 micro-rods not only effectively reduced the crystallinity of PEO-based polymers and enhanced the mobility of lithium ions, but also provided a long-range, continuous interaction surface due to their length-to-diameter ratio. Furthermore, the oxygen vacancies on the surface of 1D-TiO_2 fillers could interact with the $–CF_3$ groups in the $TFSI^-$ anion. They can alleviate ion aggregation and erratic potential gradients, make the environment uniform, and ensure the uniform deposition of lithium ions and interfacial stability. Symmetrical Li/Li batteries demonstrated a stable cycling performance of over 1000 h at 0.2 mA cm^{-2}. In addition, the 1D-TiO_2 fillers have endowed certain assembled solid lithium metal batteries, using $LiFePO_4$ as the cathode, with outstanding cycle performance (162.4 mAh g^{-1} after 200 cycles at 0.33 C) and rate performance (132 mAh g^{-1} at 2 C). Consequently, it is vindicated as a good choice to choose 1D materials with abundant surface-active sites as nanofillers. Additionally, it has been widely proven that the directional arrangement of 1D nanowires is an effective method for preparing fast ion transport paths [142–144].

3.1.3. 2D inert fillers

2D nanomaterials display features such as a high specific surface area and an ultrathin layered structure with a large aspect ratio, potentially leading to an expanded active interface area [145–147]. Moreover, these advantages would also contribute to the mechanical strength of CPEs. For example, because of its distinctive chemical and physical attributes, holey graphene oxide (HGO) was employed as a target 2D material to be incorporated into PEO-based electrolytes in Lu's research [148]. The incorporation resulted in a substantial enhancement of ionic conductivity, comparable to that of other reported ceramic and liquid electrolytes. Moreover, there was a significant improvement in the mechanical strength. Fig. 9a shows the test results of the obtained CPEs under different states such as bending, rolling, wear and torsion. Furthermore, Lu's work also demonstrated low activation energy, high Li^+ transference numbers and good stripping performance of lithium-ion coating in Li metal batteries, indicating that this CPE enhanced lithium-ion diffusion ability and electrochemical performance.

Although improvement was obtained in various performance parameters, the instability and high electrical conductivity of HGO nanosheets limited applications. Xie presented a functional nanosheet achieved through structural design and surface functionalization. This nanosheet, composed of CeO_2 and g-C_3N_4 with oxygen and nitrogen defects, established a positive charge field capable of modulating ion transport in the resulting CPE [149]. The layered structure reduced polymer crystallinity, and the surface nitrogen atoms could induce the uniform distribution of Li^+. At the same time, oxygen defects generated by rapid heating on the surface of the nanofiller were found to limit the movement of $TFSI^-$ anions and increase the migration rate of Li^+ cations in the electrolyte. The ionic conductivity of the as-prepared CPE with PEO reached 1.08×10^{-5} S cm^{-1} at room temperature, which

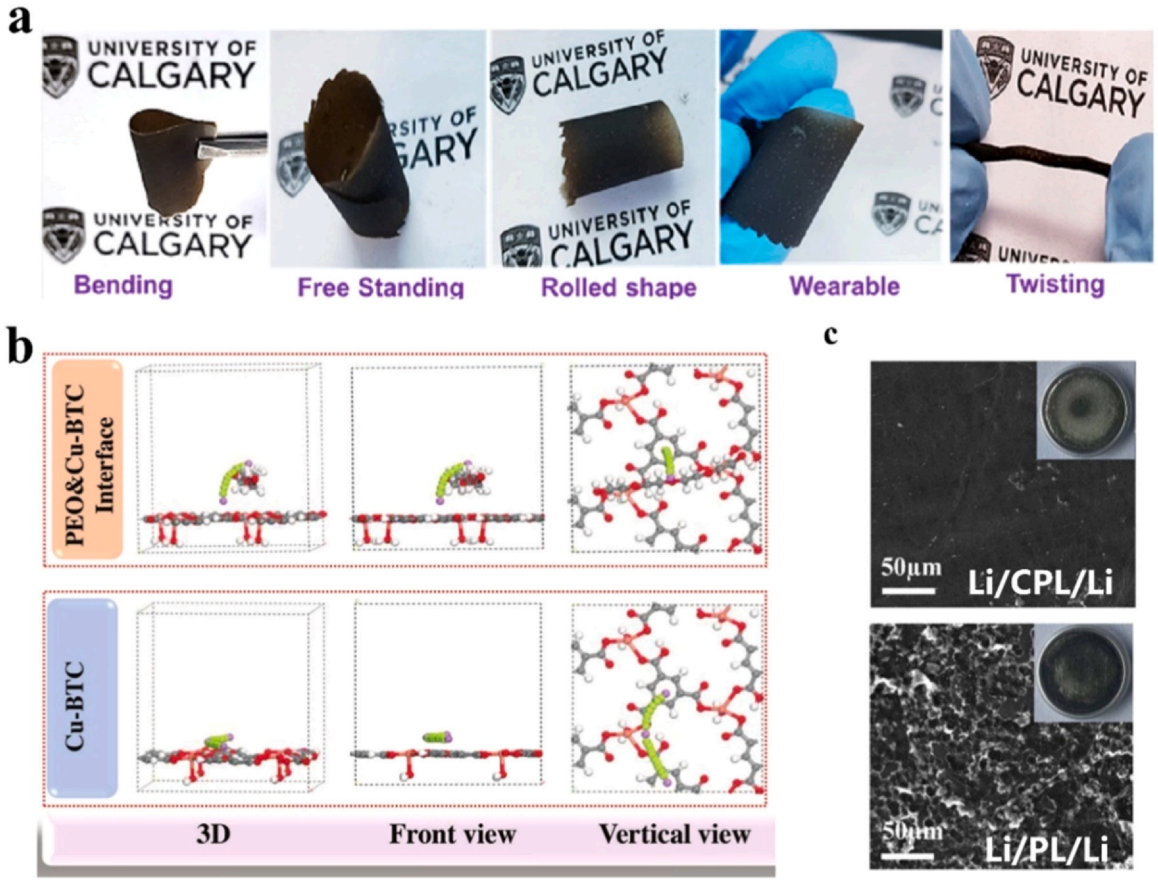

Fig. 9. a) Flexibility test of optimized CPE with different modes of application: bending, free-standing, rolling, wearing and twisting. b) Migration mechanism of Li^+ on PEO&Cu-BTC interface based on DFT. c) SEM images of the surface of Li metal electrodes in Li/8 % CPL/Li and Li/PL/Li cells during cycling after 100 cycles.(a) Reproduced with permission [148]. Copyright 2023, Elsevier. (b) Reproduced with permission [150]. Copyright 2023, Wiley-VCH. (c) Reproduced with permission [151]. Copyright 2023, Royal Society of Chemistry.

was almost 5 times that of the pure PEO electrolyte. The assembled symmetric lithium metal battery exhibited stable plating/stripping performance at a current density of 0.8 mA cm^{-2}. In addition, the final capacity of the all-solid-state $LiNi_{0.8}Co_{0.1}Mn_{0.1}O_2$/Li battery based on the CPE was 135 mAh g^{-1} after 200 cycles at 0.2 C, whilst the final capacity of the PEO/LiTFSI electrolyte system was only 42 mAh g^{-1}. By using density functional theory (DFT), Zou et al. showed that Cu-BTC with rich unsaturated metal coordination could bind with O atoms in PEO through metal-oxygen bonds, anchoring $TFSI^-$ anions and releasing Li^+, as well as introducing Li^+ into PEO as a filler material. Fig. 9b shows the migration mechanism of DFT-based Li^+ on the PEO & Cu-BTC interface and the migration mechanism of DFT-based Li^+ on Cu-BTC [150]. On this basis, 2D MOFs (Cu-BTC) with large specific surface areas and abundant active sites were synthesized, and a CPE with excellent Li^+ migration ability and ultra-stable long-period performance was constructed. The assembled symmetrical Li battery could run for 1300 h at 60 °C and 0.1 mA cm^{-2}. The assembled lithium metal solid-state battery maintained a high capacity of 162.8 mAh g^{-1} after 500 cycles at 60 °C and 0.5 C.

In terms of 2D materials, reducing the thickness of nanomaterials is an cost-effective method to achieve significant improvement with a small number of additions. Huang et al. proposed a two-dimensional, cobalt-based and ultrathin metal-organic skeleton (CMS) as a novel layered nanosheet into the PVDF/LiTFSI [151]. CMS with a high aspect ratio can effectively reduce the crystallinity of PVDF by inhibiting the regular folding arrangement between polymer chains. Moreover, a large amount of unsaturated cobalt acting as a Lewis acid can be produced in CMS, which inhibits the diffusion of $TFSI^-$ anions and promotes the transfer of Li^+. At the same time, CMS with highly symmetrical porous topology can be used as a crosslinking center in PVDF chains, forming a stable electrolyte structure. It promotes uniform deposition of lithium ions and inhibits the growth of Li dendrites. Fig. 9c shows an SEM image of a lithium metal electrode surface after 100 cycles of Li/CMS-PVDF-LiTFSI (CPL)/Li and Li/PVDF-LiTFSI (PL)/Li batteries [151]. Compared with the PL case, the lithium metal in CPL maintains a smooth surface. When the CMS load was 8 wt%, the ionic conductivity of CPL reached 6.26×10^{-4} S cm^{-1} (28 °C). As a result, the assembled symmetric Li battery exhibited a long life and stable cycling for over 750 h at 28 °C and 0.1 mA cm^{-2}. The resultant all-solid-state Li/CPL/$LiFePO_4$ battery had an ultrahigh-capacity retention rate of 99.92 % after 650 cycles at a 0.5 C rate. Besides, researchers have introduced a variety of 2D nanomaterials into the CPEs [55,152]. For instance, Zhang et al. prepared lithium montmorillonite as nanofillers to fabricate a CPE, by a simple ion-exchange method [78]. $LiFePO_4$/Li full batteries with the resulting CPE delivered a high initial discharge capacity of 145.9 mAh g^{-1} and satisfactory cycling stability with an outstanding capacity retention of 91.9 % after 200 cycles at 0.5 C and 25 °C.

It is noteworthy that the distinctive formation of 2D nanomaterials is poised to facilitate the preparation of ultrathin films, characterized by exceptional mechanical strength and flexibility. For example, Luo's group integrated few-layer vermiculite sheets into PEO-based electrolytes, yielding a thin electrolyte film characterized by a notable Young's modulus and tensile strain of ~450 % [153].

3.1.4. 3D inert fillers

To mitigate inconsistencies arising from the random distribution of inorganic fillers within an organic polymer matrix, the incorporation of

3D frameworks into polymer electrolytes emerges as an effective strategy. This approach aims to establish a continuous interface and offer mechanical support [51,154,155]. Furthermore, 3D nanostructured frameworks can promote the uniform dispersion of fillers and provide plentiful ion transmission. Up to now, versatile 3D frameworks have been applied in CPEs, i.e. bi-continuous ordered 3D structures, vertically aligned 3D frameworks, interconnected fibers with 3D architectures and porous aerogel 3D frameworks.

For example, Huang et al. introduced regenerated cellulose (RC) into PEO-based electrolytes, pioneering the development of a novel hybrid electrolyte with enhanced mechanical properties and outstanding ionic conductivity [156]. A new type of gel polymer electrolyte (PEO-RC GPEs) prepared by using RC as the coordination agent can form stable CPEs with excellent ionic conductivity, high operating voltage and enhanced safety. Thermal stability analysis has revealed that PEO-RC membrane can maintain size stability at 25–150 °C, while the original PEO-based membrane begins to shrink at 150 °C. SEM images have exhibited that the original PEO membranes have a dense structure with low porosity, negatively impacting the electrolyte penetration and absorption. In contrast, cellulose aerogels has a 3D network structure rich in micro/nanopores. The layered porous structure can provide a larger specific surface area and abundant channels, which is conducive to the absorption of electrolytes and ion migration. A large number of micro/nanopores on the surface and cross-section of the composite membrane provide pathways for lithium-ion migration, thereby enhancing battery charging/discharging retention rates.

Electrospinning is often used to prepare 3D thin frameworks. Liu et al. employed electrospinning technology to fabricate 3D γ-Al_2O_3 nanofibers, which were then incorporated into poly(vinylidene fluoride-co-hexafluoropropylene) (PVDF-HFP)-based electrolytes to prepare Al_2O_3-(PVDF-HFP) CPEs [157]. As a traditional Lewis acid, γ-Al_2O_3 nanofibers can effectively anchor LiPS through Lewis acid-base interaction, inhibiting the shuttling of LiPS, and thus enhancing the cyclic stability of sulfur cathode. In addition, Lewis's acid-base interaction between $TFSI^-$ anion and γ-Al_2O_3 nanofibers can improve the dissociation of lithium salts and promote ion conductivity and lithium-ion migration number. Furthermore, γ-Al_2O_3 can react irreversibly with any LiF produced during battery reaction processes to generate $LiAlO_2$ and Li_3AlF_6 lithium-ion conductors, further improving the ionic conductivity. Due to the increase in ionic conductivity and Li^+ transference numbers, the lithium-ion concentration gradient is greatly reduced, facilitating the uniform deposition of lithium on the anode.

The rigid 3D frameworks allow the utilization of plasticizers to improve electrochemical performance without significantly reducing mechanical properties. For instance, Xiao et al. synthesized a 3D polyimide (PI) skeleton material through electrospinning [155]. The 3D PI frameworks not only had an extremely elastic modulus enhancing their mechanical properties but also had Li dendrite blocking ability, thus improving operational safety and greatly enhancing the mechanical strength and interface stability of PEO-based electrolytes. Additionally, succinonitrile (SN) plasticizer can increase the solubility of lithium salts and inhibit the crystallization of PEO, thus significantly improving the ionic conductivity of CPE. Under the synergistic action of 3D PI frameworks and functional SN plasticizer, the ionic conductivity of PEO/LiTFSI/SN CPE reached 1.03×10^{-4} S cm^{-1}, the useful electrochemical window reached 5.14 V, and the tensile strength reached 4.52 MPa at 30 °C, which was far superior to other similar materials. Another example is provided by Du and his colleagues. An ionic liquid-confined MOF (ZIF-8)/polymer 3D layered porous membrane was prepared by electrospinning and chemical impregnation processes [158]. Due to their unique layered nano/micro-Janus structure with good surface affinity, fast Li^+ migration kinetics were obtained. The ionic conductivity was 8.17×10^{-4} S cm^{-1} at 25 °C. After 500 cycles of those assembled Li/$LiFePO_4$ cells operated at a 1 C rate, the capacity retention rate was as high as 95.3 %. The capacity only attenuated from 130 mAh g^{-1} to 124 mAh g^{-1}.

Due to the self-supporting property of 3D frameworks, several ultrathin films have been successfully developed. For example, Fan et al. used a scalable polyimide film as a reinforced 3D framework to fabricate an asymmetric CPE with an ultrathin thickness of ~20 μm. The asymmetric CPE was incorporated with a ceramic-rich layer and polymer-rich layer, enabling outstanding lithium dendrite inhibition and antioxidative stability [159]. Additionally, a bilayer CPE of 4.2 μm in thickness was constructed by introducing a porous ceramic scaffold and a double-layer Li^+-conducting polymer [160]. Therefore, Li-$Ni_{0.8}Co_{0.1}Mn_{0.1}O_2$/Li full cells delivered a high energy density of 506 Wh kg^{-1} and 1514 Wh L^{-1}. Cui's group also used an 8.6-μm-thick nanoporous polyimide film as a framework to contain PEO-based electrolytes, which exhibited an excellent dendrite inhibition ability [47]. The symmetrical lithium cells with the obtained PEO/LiTFSI thin film could prevent batteries from short-circuiting even after over 1000 h of cycling.

3.2. Active fillers

Inorganic solid electrolytes (ISEs) as active fillers can be introduced into the CPEs, inheriting the inert filler advantages while forming new Li-ion transport pathways. The additional pathways are attributed to the percolation effect involving the continuous active-filler phase and an interface phase. Therefore, using ISEs as fillers exhibits significant advantages, such as ion transport, mechanical strength, electrochemical stability and Li^+ transference numbers. So far, most inorganic electrolytes have been attempted to be introduced into CPEs, especially perovskite-type LLTO, NASICON-type LATP and LAGP, and garnet-type LLZO [54].

Compared to solid sulfide electrolytes, oxide ceramic electrolytes demonstrate enhanced stability in various solvents, thus garnering significant attention in research. Importantly, the incorporation of fillers increases residual solvent content, thereby contributing significantly to the enhancement of ionic conductivity. Notably, recent work from Zhang's group emphasized the variability in solvent adsorption capacities among different ceramic fillers, consequently influencing ionic conductivity and other electrochemical characteristics [161]. Fig. 10 provides some active fillers from 0D to 3D [70,162–164]. Different to inert fillers, these designs prefer to develop a percolation network of active fillers. From a dimensional perspective, the nanofillers with high-latitude structures exhibit more effective ion transport pathways. Additionally, the nanostructures with low-latitude structures, such as 0D or 1D materials, can also form continuous phases, thereby facilitating high ionic conductivity.

3.2.1. 0D active fillers

Most ISEs are in powder form, starting as bulk materials and reaching the desired nanoscale by mechanical ball milling. Based on the percolation effect, CPEs with nanofillers can display a higher ionic conductivity, compared with the CPEs using the micron-size active fillers. Lu et al. used LLZTO ceramic powders to mix with PVDF-HFP and LiTFSI [66]. As shown in Fig. 11a, the influence of ISE nanoparticles on the polymer crystallinity was investigated through a PVDF-HFP/LiTFSI/LLZTO CPE [66]. The CPE exhibited a high ionic conductivity of 8.80×10^{-5} S·cm^{-1} at RT, due to the reduced crystallinity of PVDF-HFP polymer matrices. Meanwhile, $LiFePO_4$/Li cells with the CPE showed excellent cycling performance with a high Coulombic efficiency of 99.6 %.

Active fillers can act as the main phase in CPEs. Wang et al. investigated the effects of PEO-based electrolytes with different molecular weights. The LAGP-PEO-500000(LiTFSI) electrolyte was proved satisfactory with a PEO content of as low as 1 wt% [165]. The resultant Li-PEO-500000(LiTFSI)/LAGP-PEO1/LiMFP full cells exhibited good cycling and rate performance. Furthermore, CPEs with LAGP as the main content were proposed, as shown in Fig. 11b [165].

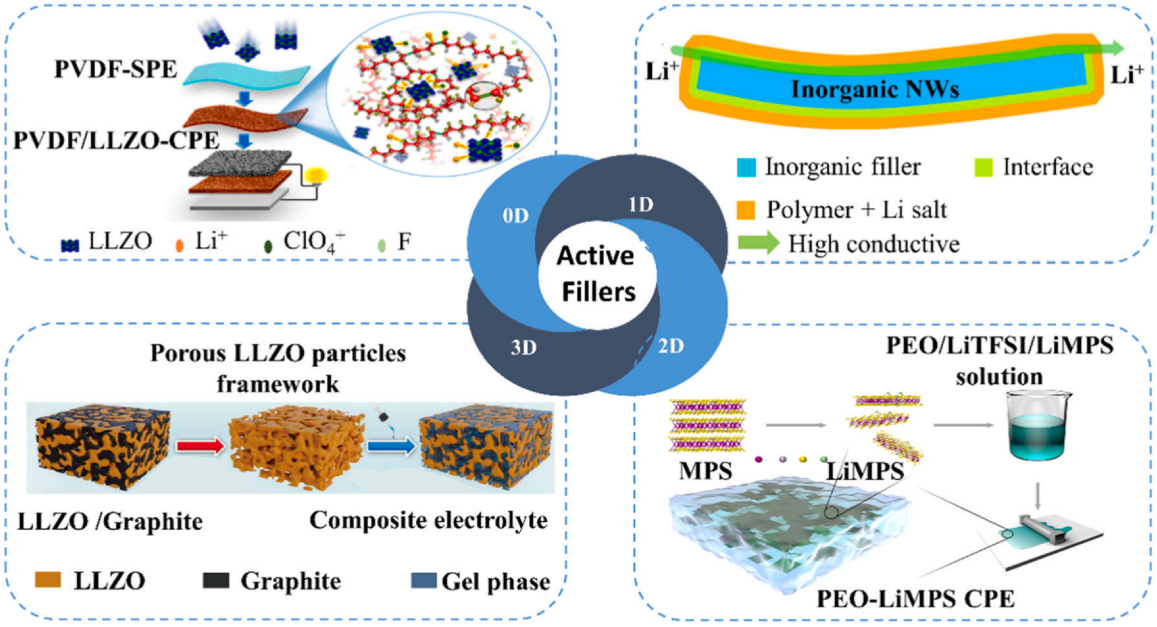

Fig. 10. Demonstration of some inorganic active fillers, with 0D, 1D, 2D and 3D geometries.Reproduced with permission [163]. Copyright 2017, American Chemical Society. Reproduced with permission [164]. Copyright 2017, Springer Nature. Reproduced with permission [70]. Copyright 2023, Elsevier. Reproduced with permission [162]. Copyright 2023, Wiley-VCH.

Besides, there are multiple interactions between active fillers and polymer-based electrolytes. For example, Zhang's group also confirmed that the addition of LLZTO particles could form a flexible anion-immobilized composite electrolyte membrane (see Fig. 11c) [64]. As a result, a $LiFePO_4$/Li cell with a specific CPE delivered a specific capacity of around 155 mAh g^{-1} with a Coulombic efficiency of 99 % and a limited polarization of 0.05 V at 0.1 C and 60 °C (see Fig. 11d and e). The assembled Li symmetrical cell also exhibited excellent stability at a current density of 0.10 mA cm^{-2} (see Fig. 11f). The interaction between polymer matrices and active fillers has also been investigated, using LLZTO ceramic particles to mix with PVDF electrolytes. The study revealed that LLZTO fillers could induce chemical dehydrofluorination in the PVDF skeleton, fostering enhanced interactions among the PVDF matrix, lithium salt and LLZTO fillers [163]. Thus, the high performance derived from the CPE was notable, exhibiting a substantial increase in ionic conductivity (approximately 5×10^{-4} S cm^{-1} at 25 °C). The resulting CPE showed high mechanical strength and favorable thermal stability.

3.2.2. 1D active fillers

Fast ionic transmission channels are desirable to form continuous ionic pathways, so research teams were motivated to develop CPEs using 1D inert fillers. Moreover, 1D active fillers are considered more likely to form a percolative network than 0D fillers. As a typical example, Cui's group used LLTO nanowires prepared by electrospinning to fabricate PAN/$LiClO_4$ electrolytes. Through incorporating 15 wt% LLTO nanowires, the composite electrolyte exhibited an unprecedented ionic conductivity of 2.4×10^{-4} S cm^{-1} at RT (Fig. 12a) [45]. In addition, the electrochemical stability window of the CPE was also enlarged by introducing the LLTO nanowires into the PAN electrolytes.

Similar to 1D inert fillers, aligned active nanowires could improve ionic conductivity compared to randomly dispersed ones. As shown in Fig. 12b, vertically aligned and interconnected LATP nanowires were engineered through an ice-templating approach [166]. This strategy resulted in an impressive ionic conductivity of 0.52×10^{-4} S cm^{-1}, showcasing a 3.6-fold improvement compared to the CPE with randomly dispersed LATP nanowires. The CPE with 1D LATP nanowires also showed high geometric stability at 180 °C and better electrochemical stability than pure SPE. Another example is provided by Cui's research group. By constructing precisely aligned inorganic Li^+-conductive nanowires, they validated the substantial enhancement in ionic conductivity in the CPE. The obtained CPE presented fast ionic conducting pathways devoid of crossings or junctions on the surfaces of the aligned LLTO nanowires in the CPEs (Fig. 12c) [164].

3.2.3. 2D active fillers

There are relatively few research reports on 2D ceramic nanosheets in CPEs [70,167–169]. Even though ISEs with 2D nanosheet structures have been synthesized less frequently, 2D active fillers still deliver some advantages. For example, graphene oxide nanosheets were used as a 2D template to successfully synthesize solid $Li_{6.5}La_3Zr_{1.5}Nb_{0.5}O_{12}$ nanosheets [168]. Similar to the inert nanosheet synthesis process, garnet precursors form co-precipitates on graphene nanosheets. The GO template was removed by subsequent air co-calcination, eventually resulting in the garnet electrolyte in the form of nanosheets. The X-ray diffraction patterns of garnet nanosheets showed the distinct crystallinity of cubic garnet. This nanosheet structure has been confirmed via transmission electron microscopy (TEM) images (Fig. 13a) [168]. 15 wt% of garnet nanosheets were composited with PEO-based electrolytes, aiming to obtain continuous Li-ions transport pathways in the CPEs. The resultant material displays a high ionic conductivity of 3.6×10^{-4} S cm^{-1} at RT. Garnet nanosheets provide a stable backbone for CPEs, which enables them to robustly inhibit Li dendrites. Thereafter, symmetric Li test batteries delivered stable reversible cycling at a current density of 0.1 mA cm^{-2} for over 200 h (at 40 °C). Those assembled $LiFePO_4$/Li full cells displayed a stable capacity at a current of 0.05 C (at 40 °C).

Recently, Wang's group reported a thin 2D laminar electrolyte with highly ordered LLTO crystals in the 2D interlayer channels of a laminar vermiculite framework, as shown in Fig. 13b and c [170]. Owing to the confinement effect of the laminar vermiculite framework, the growth of LLTO crystal was controlled into an ordered and continuous 2D arrangement with no crystal defects. More importantly, it was confirmed that the LLTO crystals grew preferentially along the c-axis in the interlayer channel, which is the fastest Li^+ transfer direction (Fig. 13d) [170]. As a result, a high ionic conductivity of 8.22×10^{-5} S cm^{-1} at 30 °C was obtained, which was higher than that of LLTO pellets, 1.77×10^{-5} S cm^{-1}. The 2D arrangement permitted the assembly of an ultrathin membrane (a thickness of 15 μm) with a compressive

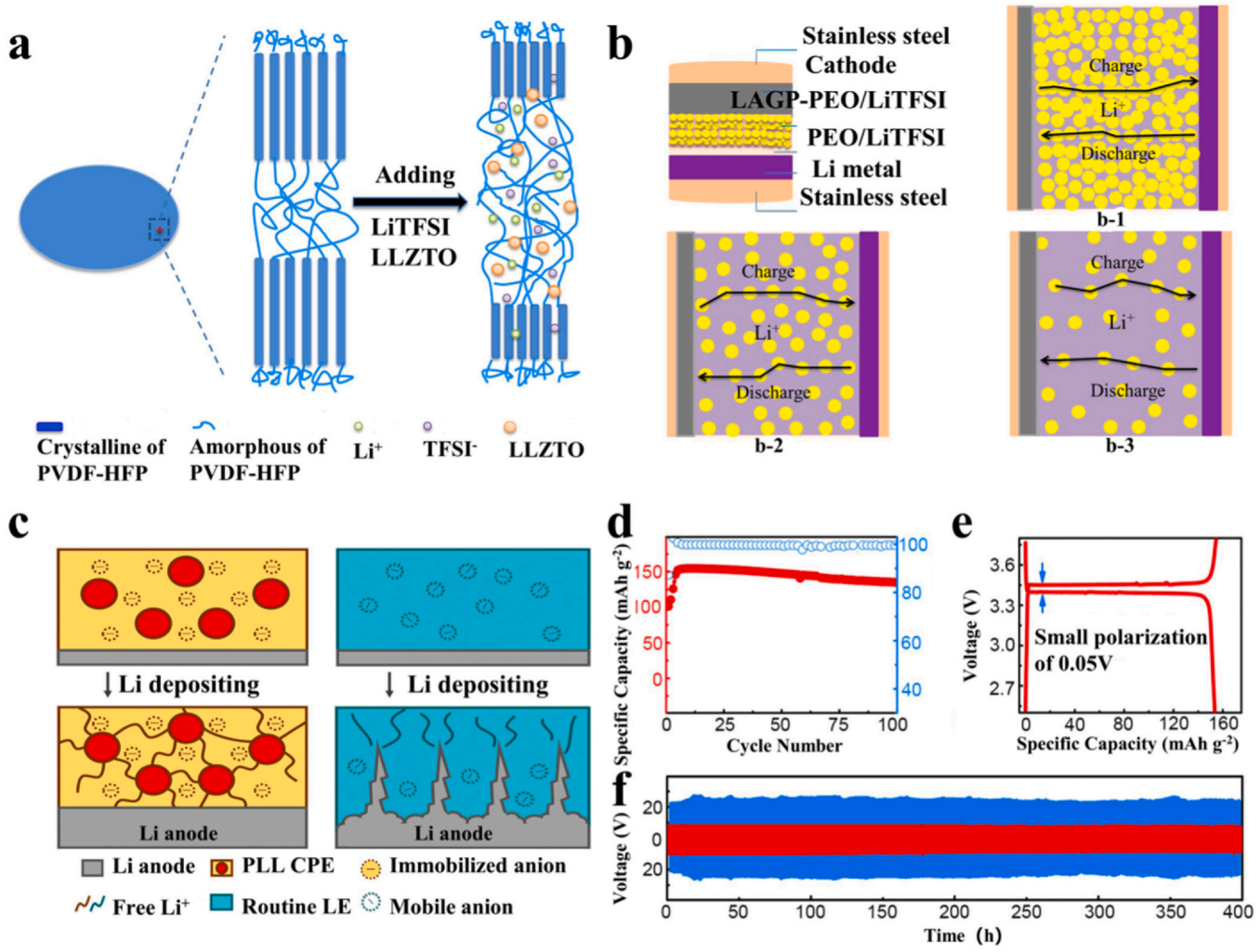

Fig. 11. a) Illustration of the effect of nanofillers on the formation of amorphous regions. b) Li^+ ion transport mechanism in CPEs with three contents of PEO. c) Schematic of immobilized anions tethered to polymer chains and LLZTO ceramic particles; d) cycling performance of an all-solid-state $LiFePO_4$/Li metal full battery and e) corresponding galvanostatic discharge/charge profile at a rate of 0.1 C and 60 °C; and f) voltage profiles of the lithium plating/stripping in a lithium symmetrical cell with PLL (60 °C, red) and routine liquid electrolytes (25 °C, blue) at a current density of 0.10 mA cm^{-2}.(a) Reproduced with permission [66]. Copyright 2019, Elsevier. (b) Reproduced with permission [165]. Copyright 2017, American Chemical Society. (f) Reproduced with permission [64]. Copyright 2017, the National Academy of Sciences.

modulus of 1.24 GPa. The resultant CPE presented a certain degree of flexibility and could be bent, while the pure garnet ceramic pieces were prone to break easily (Fig. 13e). Thus, the resultant Li/$LiFePO_4$ full battery exhibited excellent cycling performance of 149 mAh g^{-1} after 150 cycles (0.5 C, 60 °C), as shown in Fig. 13f [170].

3.2.4. 3D active fillers

As mentioned above, active fillers with 3D frameworks have been proposed not only as an effective strategy to realize continuous ion transport and high mechanical strength but also as additional interconnected ion transport networks through their ionic conductivity. Similar to inert fillers, researchers pursued 3D active fillers with a high surface area/volume ratio, to promote ion transport and electrochemical stability. Numerous works and methods have been reported to construct 3D frameworks, such as polymer templating, salt templating, spraying and electrospinning methods [171–175].

3D active networks can also be obtained by electrospinning. For example, Guo's group prepared a 3D garnet framework via the polymeric sponge method [176]. As shown in Fig. 14a, the advantages of the 3D garnet framework were proposed, including the prevention of the filler agglomeration by the 3D framework and providing continuous Li-ion transport pathways along the 3D framework. Symmetric Li metal cells based on the 3D garnet CPE demonstrated a good ability to suppress Li dendritic growth and could be cycled for over 360 h without a short circuit. The resulting CPE membrane exhibited a high ionic conductivity of 1.2×10^{-4} S cm^{-1} at 30 °C, about two times higher than that of the particle-reinforced CPEs. The assembled Li/3D garnet CPE/$LiFePO_4$ battery delivered stable cycling performance at a 0.5 C rate. Wang et al. used NaCl as a template to fabricate a 3D interconnected porous LATP framework (see Fig. 14b) [177]. Benefiting from the formation of a long-range and continuous percolation network in the 3D LATP, the ionic conductivity of the resulting CPE membrane reached 7.47×10^{-4} S cm^{-1} at 60 °C, which was higher than that of pure PEO-based electrolytes (1.0×10^{-4} S cm^{-1}). Furthermore, the mechanical properties were also enhanced by the 3D LATP frameworks. Thus, symmetric Li metal cells based on the prepared CPE showed stable cycling performance for over 1000 h at 0.2 mA cm^{-2} and 0.2 mAh cm^{-2} and for over 2000 h at 0.1 mA cm^{-2} and 0.1 mAh cm^{-2}. The assembled LFP/Li exhibited long-term stable cycling at a 1 C rate.

Moreover, Ding's group successfully constructed elastic LLZO nanofiber films with excellent alignment, as shown in Fig. 14c [178]. The resulting CPE displayed a high ionic conductivity of 1.16×10^{-4} S cm^{-1} at 30 °C with a low activation energy of 0.308 eV. The interface between the electrodes and the CPE showed good contact

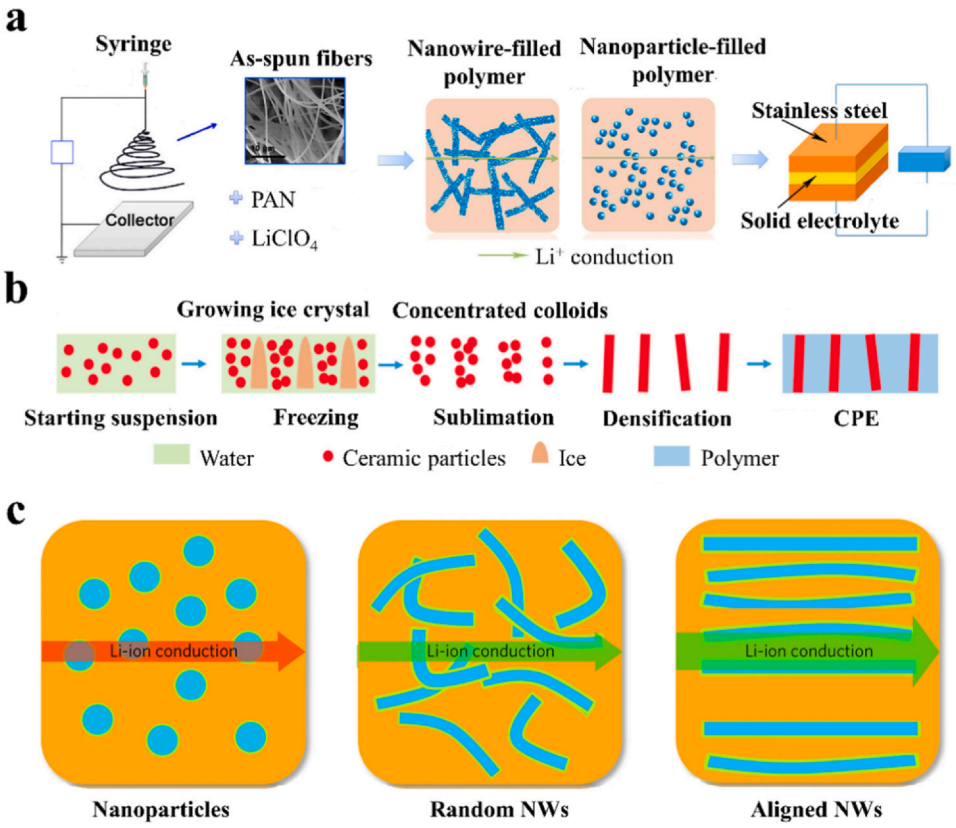

Fig. 12. a) Schematic illustration of the synthesis of 1D nanowire-filled CPE and the comparison of possible lithium-ion conduction pathways. b) Illustration of the formation process of aligned active filler nanowires. c) Comparison of possible Li-ion conduction pathways with 0D and 1D components.(a) Reproduced with permission [45]. Copyright 2015, American Chemical Society. (b) Reproduced with permission [166]. Copyright 2015, American Chemical Society. (c) Reproduced with permission [164]. Copyright 2017, Springer Nature.

continuity during repeated cycles due to the elastic surfaces of the CPEs. The resulting symmetric Li metal cells delivered stable Li plating/stripping cycling for over 700 h. A small internal resistance of 87 Ω was presented in the assembled $LiNi_{0.8}Co_{0.15}Al_{0.05}O_2$/Li cells, delivering large discharge capacities with high Coulombic efficiencies that are comparable with liquid-state batteries.

4. Rational strategies of nanocomposite design

Nanocomposite materials enable the strategic integration of fillers and polymer/Li salts, considering both dimension and size [179]. However, it is well known that nanofillers tend to aggregate/ precipitate in polymer matrices, and there are abundant grain boundaries between filler particles, especially in the 1D-3D nanocomposite active fillers. These effects contribute to the formation of monolithic blocks for continuous ion transport. Additionally, the interface compatibility between the fillers and the polymer matrices contains the concentration and the surface functional groups of fillers [180,181], the type of polymer matrices [182] and the type and the concentration of lithium salts [181,183]. All these factors affect the performance and stability of composite polymer electrolytes (CPEs) which is worth investigating.

In CPEs, the enhanced ionic conductivity largely stems from expanded interfaces between fillers and polymer matrices, coupled with intensified mutual interactions. However, these interactions may form a poor interphase layer, increasing the interfacial resistance and hindering ion transports due to the blocking effect. Multi-phase incompatibility was first observed in solid-liquid hybrid electrolyte systems, incurring some adverse chemical reactions. Jung et al. found excellent stability of $Li_{10}GeP_2S_{12}$ with the solvated ionic liquids, ascribed to the significantly reduced reactivity of the oxygen in the solvents toward nucleophilic attack on the sulfides [184]. Recently, the chemical degradation of Li_6PS_5Cl (LPSCl) induced by poly(ethylene glycol) (PEG) was revealed. As shown in Fig. 15a, the high polarity of PEG presented a continuous formation of an interface passivation layer, causing hindered Li^+ transport at the PEG/LPSCl interface [185]. The substitution of the terminal OH group in the PEG with OCH_3 terminal groups was demonstrated to not only stabilize the inner interfaces but also extend the electrochemical window of the CPEs.

In addition, grain boundaries between the fillers and the main polymer matrix can also hinder ion transport. Furthermore, nanofillers tend to agglomerate together, resulting in disconnecting the percolating network in CPEs. Recent research also demonstrated that dense nanoparticles can form ionic transport routes superior to those of porous nanoparticles (Fig. 15b) [75]. Xie et al. proposed trimethylaluminum-functionalized polyethylene oxide (PEO) electrolytes, which incorporated a high concentration of plasticizers [186]. A high ionic conductivity of 1.41 mS cm^{-1} at 30 °C was obtained. Thus, the multi-phase compatibility not only influences the ion transport properties of the solid electrolyte but also impacts the stability of the composite itself, thereby affecting the cycle stability of full cells [187].

Effective and advanced nanocomposite design should form continuous conductive lithium transport channels in CPEs at the nanoscale. Besides, some advanced nanocomposite designs have been reported to not only enhance the ionic conductivity of CPEs but also may make a significant impact on other crucial properties of CPEs, including mechanical and electrochemical properties [47,178,179,183]. Thus, the surface and morphology control of nanofillers is very important, as well as the functionalization of nanofillers, which will be reviewed in the sections following.

4.1. Size effect of fillers

To investigate the size effect of fillers, Li's group first studied Li-salt-free PEO-based composite polymer electrolytes (CPEs) mixed with different

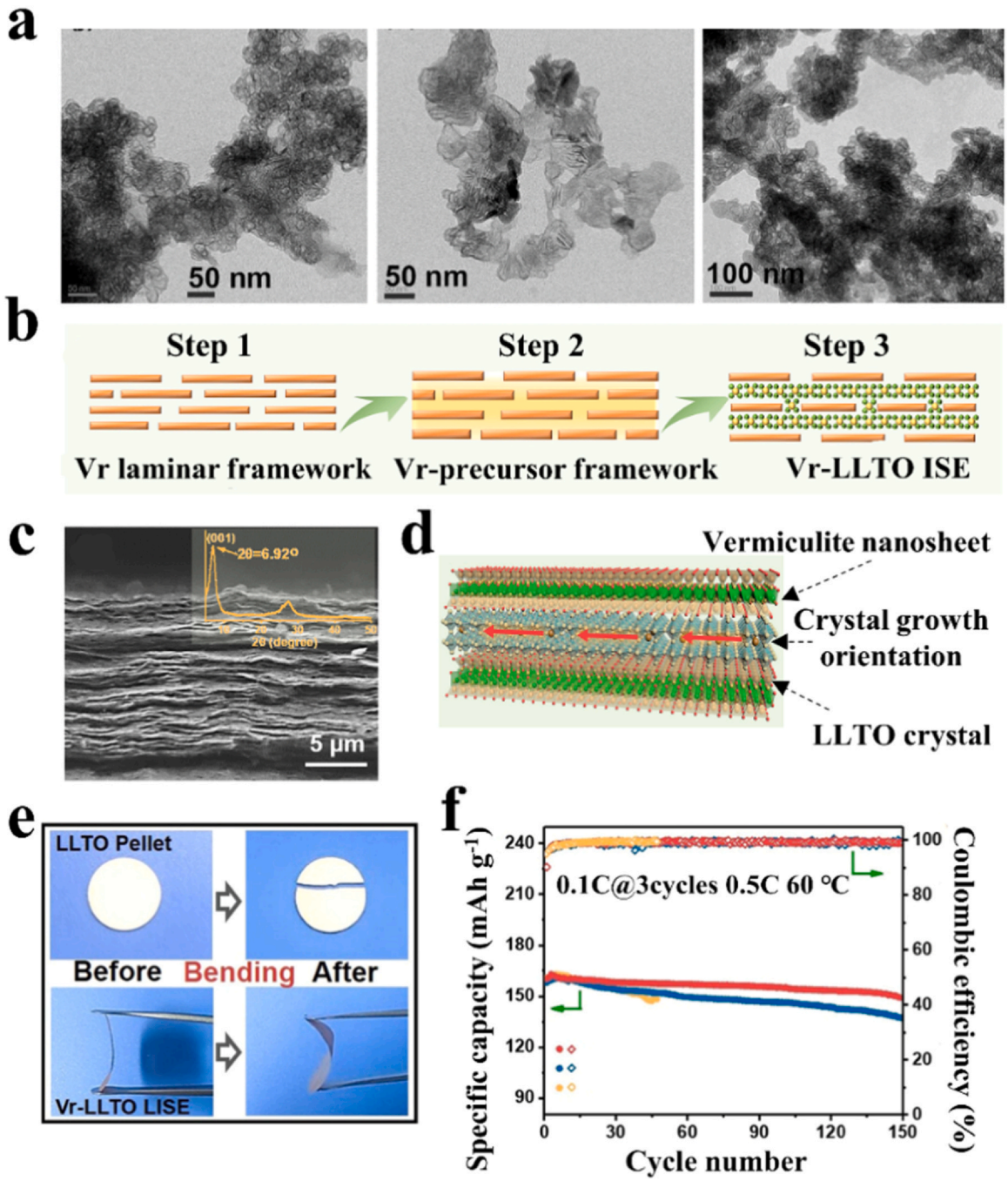

Fig. 13. a) Formation of 2D nanosheets confirmed by TEM images, with different synthesis conditions. b) Illustration of LLTO crystal growth in confined interlayer channels. c) SEM image of nanosheets. d) Schematic diagram of Li^+ transfer pathway. f) The cycling performances of the assembled full cells.(a) Reproduced with permission [168]. Copyright 2019, American Chemical Society. (f) Reproduced with permission [170]. Copyright 2022, Wiley-VCH.

LLZTO ($Li_{6.4}La_3Zr_{1.4}Ta_{0.6}O_{12}$) particles (10 μm, 400 nm and 40 nm) [188]. The results revealed that CPE with 40-nm LLZTO nanoparticles had a high ionic conductivity of 2.1×10^{-4} S cm^{-1} at 30 °C, which was nearly two orders of magnitude larger than those with the micrometer-sized particles. This case gives significant evidence for the importance of specific surface area for the dispersed active fillers, affecting the percolation effect. Those assembled $LiFePO_4$/Li and $LiFe_{0.15}Mn_{0.85}PO_4$/Li full batteries delivered good rate capability and cycling performance. Furthermore, Sun et al. studied the effect of mixed-sized fillers on CPEs [189]. Bimodal-sized LLZO ($Li_7La_3Zr_2O_{12}$) particles were introduced into PVDF–$LiClO_4$ electrolytes. The resulting CPE delivered a high ionic conductivity of 2.6×10^{-4} S cm^{-1}, which was 1 order of magnitude higher than that with nano- or micrometer-sized LLZO fillers alone.

4.2. Effect of filler concentration

The concentration of nanofillers within the CPEs plays a critical role in determining the formation of a continuous percolation network. Some previous works have investigated the difference between “ceramic-in-polymer” and “polymer-in-ceramic” concentration ranges [190,191]. As shown in Fig. 16a, PEO-LLZTO electrolytes were used to study the influence of the filler concentration [190]. The results showed that both CPEs containing 10 wt% LLZTO and 50 wt% LLZTO displayed great flexibility, while cracks were found after increasing the concentration of nanofillers up to 80 wt%. The highest ionic conductivity was found in the CPE in the ceramic-in-polymer configuration, which was greater than that of the pure PEO-LiTFSI electrolyte and those

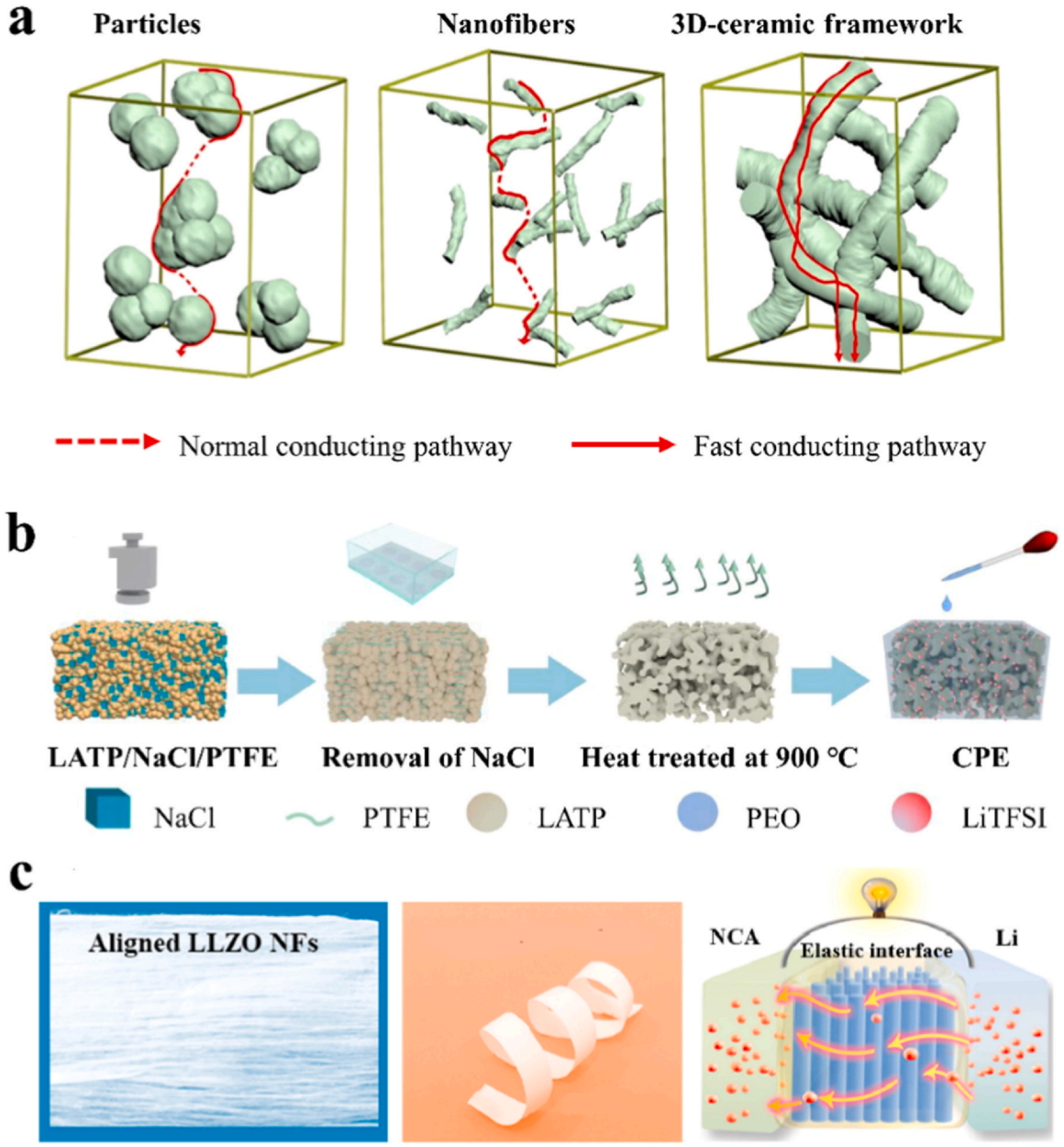

Fig. 14. a) Schematics of 3D conducting pathways in the CPEs. b) Fabrication of a 3D framework using NaCl as the template. c) Image of an aligned LLZO nanofiber membrane and illustration of the ion conduction and elastic interface of EACN/electrodes in a $LiNi_{0.8}Co_{0.15}Al_{0.05}O_2$/EACN/Li full cell.(a) Reproduced with permission [176]. Copyright 2019, American Chemical Society. (b) Reproduced with permission [177]. Copyright 2019, Elsevier. (c) Reproduced with permission [178]. Copyright 2019, Elsevier.

reported for the PEO-LiTFSI-SiO_2/ZrO_2 system. Furthermore, a "polymer-in-ceramic" membrane was easily obtained with the presence of PEG. The ionic conductivity reached 6.24×10^{-5} S cm^{-1} at 25 °C when the weight ratio of PEO:LLZTO:PEG was 10:85:5. Assembled $LiFePO_4$/Li full batteries incorporated with both "ceramic-in-polymer" and "polymer-in-ceramic" CPE types have displayed outstanding cycling stability.

Besides, the concentration of nanofillers also affects the interface compatibility between SSEs and electrodes. Guo's group utilized the nanoparticle sedimentation in polymer to prepare a heterogeneous multilayered solid electrolyte (HMSE), which could effectively broaden the electrochemical stability window of the CPEs to 0–5 V. Additionally, flexible PAN@LAGP (80 wt%) CPEs of a Janus construction type have also been obtained (see Fig. 16b) [192]. The resulting $LiNi_{0.6}Co_{0.2}Mn_{0.2}O_2$/Li and $LiNi_{0.8}Co_{0.1}Mn_{0.1}O_2$/Li batteries delivered high capacity and long cycle life. To investigate the mechanism of the improved ionic conductivity from the concentration of nanofillers, Zheng et al. used solid-state Li NMR with a ^{6}Li-^{7}Li isotope-replacement strategy to investigate lithium-ion transport pathways within LLZO-PEO/LiTFSI electrolytes (Fig. 16c) [183]. From the NMR results, they confirmed that Li ions mainly passed through the PEO polymer matrix (along the interface), and no percolated network was formed in LLZO (5 and 20 wt%)-PEO (LiTFSI) CPE. In contrast, the formation of a connected LLZO percolation network was detected in LLZO (50 wt%)-PEO (LiTFSI) CPE, which could support additional Li^+ diffusion. Therefore, the concentration of nanofillers in the CPEs influences the formation of a percolation network, interface compatibility, mechanical properties and electrochemical compatibility.

4.3. Functional design for multiphase interface compatibility

As mentioned above, the interface compatibility between polymer/Li salt electrolytes and fillers is critical for the cycling stability of CPEs

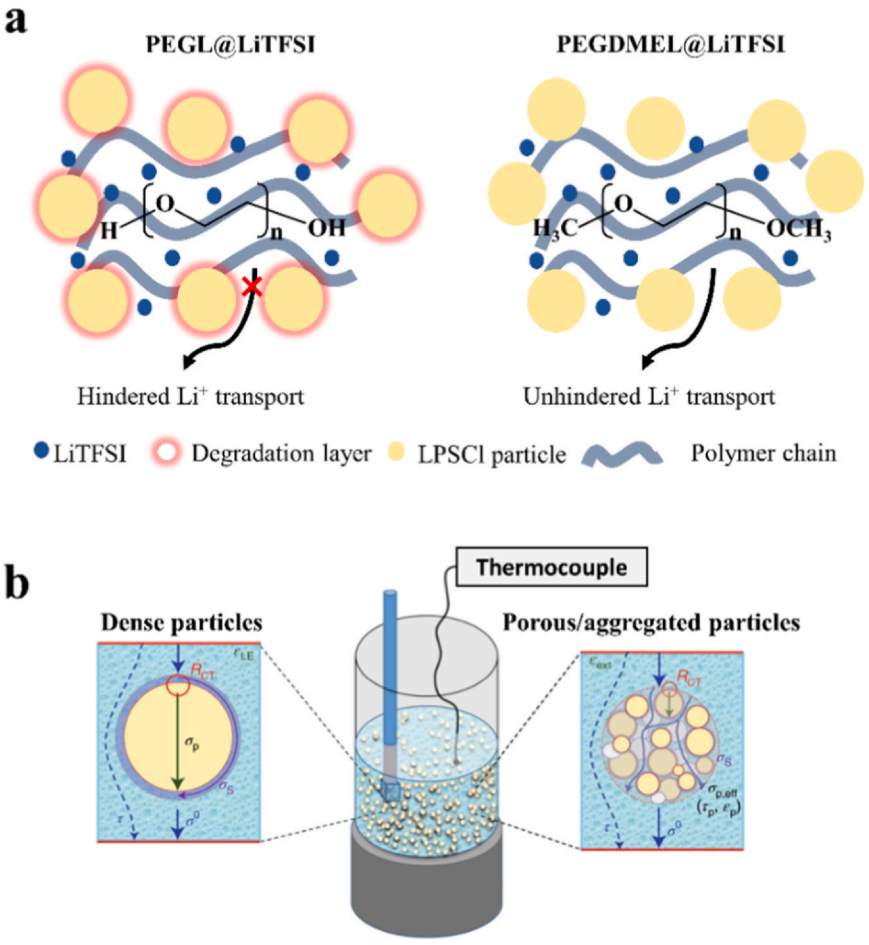

Fig. 15. a) Schematics of the different interface chemistry in PEGL@LiTFSI and PEGDMEL@LiTFSI. b) Comparison of possible factors for effective conductivity in CPEs and liquid electrolytes.(a) Reproduced with permission [185]. Copyright 2023, Wiley-VCH. (b) Reproduced with permission [75]. Copyright 2022, Springer Nature.

in solid-state lithium metal batteries (SSLMBs). At present, this aspect is receiving extensive attention and research [194–198]. Previous studies have focused on the functional design of the nanofiller, which was helpful for the stability of the nanofiller phase in the CPEs [199–208].

As an illustration, Huang et al. introduced a nanometer-scale, self-assembled monolayer protection system designed to suppress interfacial side reactions on LLZO ($Li_7La_3Zr_2O_{12}$) materials within common liquid-state electrolyte systems [209]. Typically, a minimal quantity of organic liquid electrolyte was injected into the interface of SSE/electrodes, leading to a reduction of interfacial resistances. However, undesirable Li^+/H^+ ion exchange and the formation of LiOH on LLZO particles were observed in the hybrid LLZO/liquid electrolyte system, representing the initial steps of the decomposition process. To address this, treatment with a solution of 4-chlorobenzoic acid (CBA) in isopropanol solvents resulted in the formation of a self-assembled monolayer that effectively prevented the side reaction between LLZO and liquid-state electrolytes. The LLZO-CBA presented an ultrathin solid-liquid electrolyte interphase, contrasting with the thick interphase layer exceeding 15 nm on the pristine LLZO surface. Those assembled Li/$LiFePO_4$ full cells delivered a remarkable improvement of over 39 % in specific energy after 600 cycles. Additionally, the resulting critical current density of symmetric lithium metal cells doubled to 4.6 mA cm^{-2}.

In another study, Shim et al. utilized perfluoropolyether-functionalized BN nanofibers (FBN) to increase the surface area and compatibility with PVDF-HFP polymers [210]. The FBN, prepared by sonication-assisted exfoliation and noncovalent functionalization of nano-sized BN powders maintained the 2D morphology of BN with a thickness of 3–4 nm. The resultant membrane exhibited a porous structure due to the presence of FBN. The obtained membrane showed greatly enhanced overall electrochemical and physical properties, including ionic conductivity, Li^+ transference numbers and mechanical modulus. Thus, the assembled symmetric Li metal cells showed an unprecedentedly long charging/discharging cycling time of 1940 h at a high current density of 1 mA cm^{-2}.

With further development, researchers have begun to pay more attention to the stability and effectiveness of multiphase interfaces in the CPEs [211–217]. Zhang's group reported a flexible PEO/PEG-3$Li_{10}GeP_2S_{12}$ electrolyte via an in-situ coupling reaction [218]. To enhance the compatibility of PEO-based electrolytes and $Li_{10}GeP_2S_{12}$ fillers, a chemical bonding interaction was established by utilizing (3-chloropropyl) trimethoxy silane (CTMS) as a bridge builder. The CTMS facilitated chemical bonding interaction between inorganic $Li_{10}GeP_2S_{12}$ and organic PEO polymers. The introduction of PEG provided additional –OH groups for chemical bonding with CTMS. The as-prepared CPE membrane exhibited a notable ionic conductivity of 9.83×10^{-4} S cm^{-1} at RT and a high Li^+ transference number of 0.68. This membrane demonstrated stable cycling of symmetric lithium cells over 6700 h at RT. Those assembled $LiFePO_4$/Li full cells also delivered good electrochemical performance, high-capacity retention and stable Coulombic efficiency. Recently, Kondori et al. used PEO-$Li_{10}GeP_2S_{12}$ electrolytes in a lithium-air battery investigation [219]. The as-prepared CPE facilitated a four-electron redox reaction involving lithium oxide (Li_2O) formation and decomposition, enabling stable cycling for 1000 cycles with a low polarization gap at a high rate (at RT) that operated in the air. Benefited by the CPEs, those assembled solid-state lithium-air

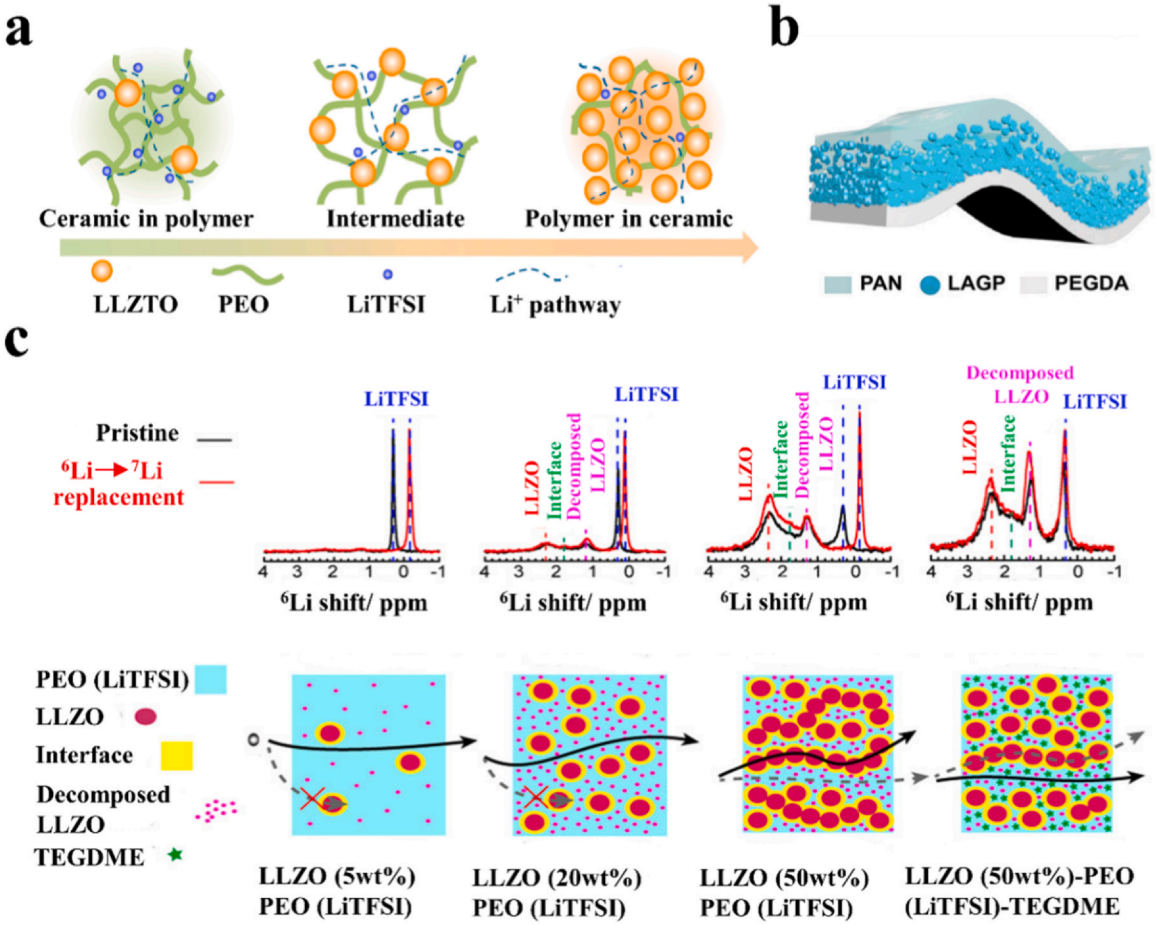

Fig. 16. a) Schematic illustration for different concentrations of nanofillers, including "ceramic-in-polymer", "intermediate" and "polymer-in-ceramic." b) Schematic diagram of HMSE with a Janus construction. c) Schematic of Li-ion pathways within three different LLZO contents in the CPEs.(a) Reproduced with permission [190]. Copyright 2018, Elsevier. (b) Reproduced with permission [192]. Copyright 2023, Wiley-VCH. (c) Reproduced with permission [193]. Copyright 2018, American Chemical Society.

batteries achieved a capacity of up to ~10.4 mAh cm^{-2}, resulting in a specific energy of ~685 Wh kg^{-1} for each cell.

In another work, Yi et al. focused on the dehydrofluorination phenomenon of PVDF-HFP electrolytes incorporating LLZO [220]. The LLZO surfaces were precisely phosphatized by a surface Li_2CO_3 mediated chemical reaction, resulting in a neutral chemical environment on the LLZO surfaces. This design not only realized the uniform distribution of ceramic and polymer phases but also provided high-throughput ion percolation pathways, enhancing ionic conductivity and Li^+ transference numbers. Besides these effects, the conformal Li_3PO_4 layer created on the LLZTO surface was helpful for the distribution of the LLZTO fillers, which endowed excellent elasticity (250 %). A sufficient ionic conductivity of 1.9×10^{-4} S cm^{-1} was achieved in the as-prepared CPE with a wide electrochemical stability window of up to 5 V vs Li^+/Li. The phosphatized layer on the LLZO surface also formed robust Li_3P-containing SEI, which significantly inhibited lithium penetration in the CPE. Thus, symmetric Li metal cells demonstrated stable cycling performance for approximately 1000 h. Those assembled Li/$LiFePO_4$ and Li/$LiNi_{0.8}Co0.1Mn_{0.1}O_2$ full cells delivered outstanding cycling performance at RT.

The functional design has also been shown to optimize electrode loading and rate performance. Kang's group constructed $BaTiO_3$–LLTO nanowires with a side-by-side heterojunction structure (PVBL) to overcome the low ionic conductivity challenge of CPEs [53]. In this case, the polarized dielectric $BaTiO_3$ greatly promoted the dissociation of Li salts to produce more movable lithium ions, which could locally and spontaneously transfer across the interface of the PVBL nanowires to couple LLTO for highly efficient ion transport. The heterojunction structure of $BaTiO_3$- LLTO nanowires effectively restrained the formation of space charge layers with PVDF. The CPEs with PVBL fillers showed a quite high ionic conductivity (8.2×10^{-4} S cm^{-1}) and a high Li+ transference number of 0.57 at 25 °C. Moreover, the interfacial electric field with electrodes was homogenized by the PVBL nanowires. The as-prepared $LiNi_{0.8}Co_{0.1}Mn_{0.1}O_2$/Li full batteries displayed a stable cycling performance of 1500 times at a current density of 180 mA g^{-1}. The test batteries in pouch formation exhibited excellent electrochemical and safety performance.

In addition to enhancing ionic conductivity and interface compatibility of resultant CPEs, researchers have also pursued strategies to enhance the thermal stability of composite electrolytes through functionalized nanocomposite materials. Considerable attention has been paid to exploring nanocomposite materials with porous structures for loading ionic liquids as fillers in the CPEs [221]. The immobilized ionic liquids within nanoporous materials exhibit exceptional thermal stability, thereby ensuring that the resulting CPE maintains high ionic conductivity and interface compatibility while preserving its excellent mechanical properties [222]. Additionally, the development of polymer substrates with inherent flame-retardant properties holds promise as an effective improvement strategy [223].

Recently, Huang's group incorporated a reactive flame-retardant unit (Br) into the polyurethane framework via covalent bonding, resulting in outstanding nonflammability properties [224]. Uniform dispersion of flame-retardant functional groups within the electrolyte can also be achieved through nanocomposite design, further contributing to enhanced thermal stability [225,226]. For instance, Guo et al.

introduced Al-MOF nanomaterials with high-temperature stable microporous structures and abundant Al^{3+} coordination sites as fillers to construct a nonflammable electrolyte. The $LiFePO_4$/Li full cells with this nonflammable electrolyte showed significant cycling stability for 200 cycles with a capacity retention of 90 % and an average Coulombic efficiency of 99 % at 120 °C [227]. Thus, the incorporated flame-retardant reagents or functional groups can be uniformly distributed within the CPEs through nanocomposite design, indicating the versatility of nanocomposite functionalization.

5. Concluding remarks and future prospects

In comparison with traditional inorganic solid electrolytes (ISEs) and solid polymer electrolytes (SPEs), composite polymer electrolytes (CPEs) offer a multitude of benefits, especially when it comes to the practical application in solid-state lithium metal batteries (SSLMBs). Researchers have dedicated significant efforts to understanding the impact of filler characteristics, such as size, dimension, concentration and interfacial compatibility, for creating interfaces that enable rapid ion transport. The benefits of nanocomposite design for CPEs at the nanoscale have prominently emerged in these systems. The fundamental mechanisms for enhancing the performance of CPEs have been widely investigated, and we have summarized two aspects in detail. Firstly, this review has covered common composite electrolyte designs and elucidated the mechanisms of beneficial effects of composite polymer electrolytes on ionic conductivity and transport pathways. We have emphasized the necessity and progress of nanocomposite designs for fabricating high-performance CPEs. Secondly, the fundamental mechanism of interface compatibility was summarized, which includes not only the compatibility of the electrolyte-electrode interface but also the interfacial compatibility between THE nanofillers and the polymer-Li salts. It should be noted that, due to the complexity and diversity of components integrated through various design strategies, there is currently no unanimous consensus on some of the theoretical mechanisms proposed.

Nevertheless, it is widely acknowledged that the introduction of fillers can improve the properties of CPEs, and this has been proven by most reported studies. The above-mentioned mechanisms aid in classifying composite materials and designing strategies. Scientists are pursuing the construction of abundant and uniform fast ion transport paths at continuous interfaces by advanced nanocomposite strategies, which could promote the ion conductivity of CPEs to reach the required level. Well-designed CPEs can not only attain high ion conductivity comparable to that of common liquid electrolytes at temperatures of interest, but also attain high safety and high energy density levels that their counterparts cannot reach.

However, despite significant advancements, the large-scale practical application of CPEs still has some remaining challenges at present. On the one hand, improved ionic conductivity and interfacial stability of CPEs relative to the SPEs both need to be further improved, although it seems very close to practical application. The ionic conductivity of the CPEs is expected to match with the fast ionic conductors. On the other hand, further in-depth research should be conducted to improve the long-term stability of the interfacial contacts for CPEs. Furthermore, some CPE performances in full batteries need further improvements, such as high loading of electrode materials, high safety, ultrathin electrolyte design and long cycling stability. Moving forward, the envisioned prospects are outlined as follows:

1) Strategically designing nanocomposite electrolytes presents a promising approach to attain room-temperature ion conductivity levels comparable to those of liquid electrolytes and inorganic solid-state ion conductors. This necessitates novel and systematical manipulation of the dimensions, size, concentration and composite forms of nanomaterials.
2) Achieving long-term stable interface compatibility is crucial for ensuring the cycle stability of full batteries. While certain advanced nanocomposite designs have successfully achieved stable integration of multiple phases, challenges persist at the interfaces within CPEs, necessitating further refinement. The performance of CPEs is subject to variation due to dynamic changes in the complex internal interfacial environments, which are influenced by chemical, electrochemical and mechanochemical effects. Addressing these challenges calls for innovative functional design strategies aimed at achieving desirable properties, such as self-healing capabilities and high lithium-ion transference numbers.
3) In contrast to commercial lithium-ion batteries (LIBs), special attention must be given to the loading of active electrode materials in solid-state lithium metal batteries (SSLMBs). Composite electrodes, typically used in SSLMBs, can lead to either increased electrode thickness or decreased loading of active materials. Additionally, employing liquid electrolytes to enhance interfacial wetting inadvertently reintroduces issues characteristic of liquid electrolytes, such as safety concerns and reduced energy density.
4) The safety risk associated with lithium dendrite growth remains a challenge in CPEs. The capacity of CPEs to prevent dendrite formation and growth reduces over successive lithium plating and stripping cycles. Additionally, the effectiveness of CPEs in hindering lithium dendrite proliferation is limited. The behavior of lithium deposition and electroplating under high current densities and substantial capacities may fall short of practical application standards.
5) The thickness of most SSEs currently stands at approximately 100 μm. There is an urgent need to advance the development of preparation technologies for ultrathin electrolyte layers to enhance the energy density of full cells.
6) In the end, the long-term cycling performance of full batteries is the main criterion for evaluating whether the battery can be practically used. It is worth noting that the pursuit of long-cycle performance, especially with batteries featuring high-capacity cathode materials, remains a paramount goal within the industry. Presently, most studies have focused on using $LiFePO_4$ as the cathode material, which stands as the predominant choice for solid-state electrolytes.

Declaration of Competing Interest

The authors declare that they have no known competing financial interests or personal relationships that could have appeared to influence the work reported in this paper.

Acknowledgments

G. Wang would like to acknowledge the support from the Australian Research Council (ARC) through the Discovery Projects (DP210101389 and DP230101579), ARC Linkage Project (LP200200926) and the ARC Research Hub for Integrated Energy Storage Solutions (IH180100020). M. Yao would like to acknowledge the support from Sichuan Science and Technology Program (No: 2021YFG0283) and the Fundamental Research Funds for the Central Universities (No: YJ202280).

References

[1] M. Winter, B. Barnett, K. Xu, Before Li ion batteries, Chem. Rev. 118 (2018) 11433–11456, https://doi.org/10.1021/acs.chemrev.8b00422.
[2] T.M. Gür, Review of electrical energy storage technologies, materials and systems: challenges and prospects for large-scale grid storage, Energy Environ. Sci. 11 (2018) 2696–2767, https://doi.org/10.1039/C8EE01419A.
[3] O. Schmidt, S. Melchior, A. Hawkes, I. Staffell, Projecting the future levelized cost of electricity storage technologies, Joule 3 (2019) 81–100, https://doi.org/10.1016/j.joule.2018.12.008.
[4] M. Li, J. Lu, Z. Chen, K. Amine, 30 Years of lithium-ion batteries, Adv. Mater. 30 (2018) 1800561, https://doi.org/10.1002/adma.201800561.
[5] F. Wu, J. Maier, Y. Yu, Guidelines and trends for next-generation rechargeable lithium and lithium-ion batteries, Chem. Soc. Rev. 49 (2020) 1569–1614, https://doi.org/10.1039/C7CS00863E.
[6] K. Qin, K. Holguin, M. Mohammadiroudbari, J. Huang, E.Y.S. Kim, R. Hall, C. Luo, Strategies in structure and electrolyte design for high-performance lithium metal batteries, Adv. Funct. Mater. 31 (2021) 2009694, https://doi.org/10.1002/adfm.202009694.

[7] X.-B. Cheng, C.-Z. Zhao, Y.-X. Yao, H. Liu, Q. Zhang, Recent advances in energy chemistry between solid-state electrolyte and safe lithium-metal anodes, Chem 5 (2019) 74–96, https://doi.org/10.1016/j.chempr.2018.12.002.
[8] J. Xiao, F. Shi, T. Glossmann, C. Burnett, Z. Liu, From laboratory innovations to materials manufacturing for lithium-based batteries, Nat. Energy 8 (2023) 329–339, https://doi.org/10.1038/s41560-023-01221-y.
[9] S. Zhou, J. Shi, S. Liu, G. Li, F. Pei, Y. Chen, J. Deng, Q. Zheng, J. Li, C. Zhao, I. Hwang, C.-J. Sun, Y. Liu, Y. Deng, L. Huang, Y. Qiao, G.-L. Xu, J.-F. Chen, K. Amine, S.-G. Sun, H.-G. Liao, Visualizing interfacial collective reaction behaviour of Li-S batteries, Nature 621 (2023) 75–81, https://doi.org/10.1038/s41586-023-06326-8.
[10] H. Li, H. Yang, X. Ai, Routes to electrochemically stable sulfur cathodes for practical Li-S batteries, Adv. Mater. (2023) 2305038, https://doi.org/10.1002/adma.202305038.
[11] Z. Liang, W. Wang, Y.-C. Lu, The path toward practical Li-air batteries, Joule 6 (2022) 2458–2473, https://doi.org/10.1016/j.joule.2022.10.008.
[12] X. Chi, M. Li, J. Di, P. Bai, L. Song, X. Wang, F. Li, S. Liang, J. Xu, J. Yu, A highly stable and flexible zeolite electrolyte solid-state Li-air battery, Nature 592 (2021) 551–557, https://doi.org/10.1038/s41586-021-03410-9.
[13] H. Wang, Z. Yu, X. Kong, S.C. Kim, D.T. Boyle, J. Qin, Z. Bao, Y. Cui, Liquid electrolyte: the nexus of practical lithium metal batteries, Joule 6 (2022) 588–616, https://doi.org/10.1016/j.joule.2021.12.018.
[14] X. Chen, B. Zhao, C. Yan, Q. Zhang, Review on Li deposition in working batteries: from nucleation to early growth, Adv. Mater. 33 (2021) 2004128, https://doi.org/10.1002/adma.202004128.
[15] J. Zheng, M.S. Kim, Z. Tu, S. Choudhury, T. Tang, L.A. Archer, Regulating electrodeposition morphology of lithium: towards commercially relevant secondary Li metal batteries, Chem. Soc. Rev. 49 (2020) 2701–2750, https://doi.org/10.1039/C9CS00883G.
[16] Y. Meng, D. Zhou, R. Liu, Y. Tian, Y. Gao, Y. Wang, B. Sun, F. Kang, M. Armand, B. Li, G. Wang, D. Aurbach, Designing phosphazene-derivative electrolyte matrices to enable high-voltage lithium metal batteries for extreme working conditions, Nat. Energy 8 (2023) 1023–1033, https://doi.org/10.1038/s41560-023-01339-z.
[17] A. Yang, C. Yang, K. Xie, S. Xin, Z. Xiong, K. Li, Y.-G. Guo, Y. You, Benchmarking the safety performance of organic electrolytes for rechargeable lithium batteries: a thermochemical perspective, ACS Energy Lett. 8 (2023) 836–843, https://doi.org/10.1021/acsenergylett.2c02683.
[18] M. Li, C. Wang, Z. Chen, K. Xu, J. Lu, New concepts in electrolytes, Chem. Rev. 120 (2020) 6783–6819, https://doi.org/10.1021/acs.chemrev.9b00531.
[19] S. Xin, Y. You, S. Wang, H.-C. Gao, Y.-X. Yin, Y.-G. Guo, Solid-state lithium metal batteries promoted by nanotechnology: progress and prospects, ACS Energy Lett. 2 (2017) 1385–1394, https://doi.org/10.1021/acsenergylett.7b00175.
[20] J. Lopez, D.G. Mackanic, Y. Cui, Z. Bao, Designing polymers for advanced battery chemistries, Nat. Rev. Mater. 4 (2019) 312–330, https://doi.org/10.1038/s41578-019-0103-6.
[21] S. Xia, X. Wu, Z. Zhang, Y. Cui, W. Liu, Practical challenges and future perspectives of all-solid-state lithium-metal batteries, Chem 5 (2019) 753–785, https://doi.org/10.1016/j.chempr.2018.11.013.
[22] Y. Zheng, Y. Yao, J. Ou, M. Li, D. Luo, H. Dou, Z. Li, K. Amine, A. Yu, Z. Chen, A review of composite solid-state electrolytes for lithium batteries: fundamentals, key materials and advanced structures, Chem. Soc. Rev. 49 (2020) 8790–8839, https://doi.org/10.1039/D0CS00305K.
[23] Q. Zhao, S. Stalin, C.-Z. Zhao, L.A. Archer, Designing solid-state electrolytes for safe, energy-dense batteries, Nat. Rev. Mater. 5 (2020) 229–252, https://doi.org/10.1038/s41578-019-0165-5.
[24] J. Janek, W.G. Zeier, Challenges in speeding up solid-state battery development, Nat. Energy 8 (2023) 230–240, https://doi.org/10.1038/s41560-023-01208-9.
[25] P. Lennartz, B.A. Paren, A. Herzog-Arbeitman, X.C. Chen, J.A. Johnson, M. Winter, Y. Shao-Horn, G. Brunklaus, Practical considerations for enabling Li|polymer electrolyte batteries, Joule 7 (2023) 1471–1495, https://doi.org/10.1016/j.joule.2023.06.006.
[26] R. Chen, Q. Li, X. Yu, L. Chen, H. Li, Approaching practically accessible solid-state batteries: stability issues related to solid electrolytes and interfaces, Chem. Rev. 120 (2020) 6820–6877, https://doi.org/10.1021/acs.chemrev.9b00268.
[27] A. Banerjee, X. Wang, C. Fang, E.A. Wu, Y.S. Meng, Interfaces and interphases in all-solid-state batteries with inorganic solid electrolytes, Chem. Rev. 120 (2020) 6878–6933, https://doi.org/10.1021/acs.chemrev.0c00101.
[28] Y.-C. Yin, J.-T. Yang, J.-D. Luo, G.-X. Lu, Z. Huang, J.-P. Wang, P. Li, F. Li, Y.-C. Wu, T. Tian, Y.-F. Meng, H.-S. Mo, Y.-H. Song, J.-N. Yang, L.-Z. Feng, T. Ma, W. Wen, K. Gong, L.-J. Wang, H.-X. Ju, Y. Xiao, Z. Li, X. Tao, H.-B. Yao, A $LaCl_3$-based lithium superionic conductor compatible with lithium metal, Nature 616 (2023) 77–83, https://doi.org/10.1038/s41586-023-05899-8.
[29] W. Xia, Y. Zhao, F. Zhao, K. Adair, R. Zhao, S. Li, R. Zou, Y. Zhao, X. Sun, Antiperovskite electrolytes for solid-state batteries, Chem. Rev. 122 (2022) 3763–3819, https://doi.org/10.1021/acs.chemrev.1c00594.
[30] C. Wang, J.T. Kim, C. Wang, X. Sun, Progress and prospects of inorganic solid-state electrolyte-based all-solid-state pouch cells, Adv. Mater. 35 (2023) 2209074, https://doi.org/10.1002/adma.202209074.
[31] H. Liu, Y. Liang, C. Wang, D. Li, X. Yan, C. Nan, L. Fan, Priority and prospect of sulfide-based solid-electrolyte membrane, Adv. Mater. 35 (2023) 2206013, https://doi.org/10.1002/adma.202206013.
[32] X. Li, J. Liang, X. Yang, K.R. Adair, C. Wang, F. Zhao, X. Sun, Progress and perspectives on halide lithium conductors for all-solid-state lithium batteries, Energy Environ. Sci. 13 (2020) 1429–1461, https://doi.org/10.1039/C9EE03828K.
[33] Q. Zhou, J. Ma, S. Dong, X. Li, G. Cui, Intermolecular chemistry in solid polymer electrolytes for high-energy-density lithium batteries, Adv. Mater. 31 (2019) 1902029, https://doi.org/10.1002/adma.201902029.
[34] S. Zhou, S. Zhong, Y. Dong, Z. Liu, L. Dong, B. Yuan, H. Xie, Y. Liu, L. Qiao, J. Han, W. He, Composition and structure design of poly(vinylidene fluoride)-based solid polymer electrolytes for lithium batteries, Adv. Funct. Mater. 33 (2023) 2214432, https://doi.org/10.1002/adfm.202214432.
[35] Z. Xue, D. He, X. Xie, Poly(ethylene oxide)-based electrolytes for lithium-ion batteries, J. Mater. Chem. A 3 (2015) 19218–19253, https://doi.org/10.1039/C5TA03471J.
[36] J. Pan, P. Zhao, N. Wang, F. Huang, S. Dou, Research progress in stable interfacial constructions between composite polymer electrolytes and electrodes, Energy Environ. Sci. 15 (2022) 2753–2775, https://doi.org/10.1039/D1EE03466A.
[37] Y. Chen, K. Wen, T. Chen, X. Zhang, M. Armand, S. Chen, Recent progress in all-solid-state lithium batteries: the emerging strategies for advanced electrolytes and their interfaces, Energy Storage Mater. 31 (2020) 401–433, https://doi.org/10.1016/j.ensm.2020.05.019.
[38] J. Weston, B. Steele, Effects of inert fillers on the mechanical and electrochemical properties of lithium salt-poly(ethylene oxide) polymer electrolytes, Solid State Ion. 7 (1982) 75–79, https://doi.org/10.1016/0167-2738(82)90072-8.
[39] W. Wieczorek, K. Such, H. Wycilik, Modifications of crystalline structure of peo polymer electrolytes with ceramic additives, Solid State Ion. 36 (1989) 255–257, https://doi.org/10.1016/0167-2738(89)90185-9.
[40] F. Croce, G.B. Appetecchi, L. Persi, B. Scrosati, Nanocomposite polymer electrolytes for lithium batteries, Nature 394 (1998) 456–458, https://doi.org/10.1038/28818.
[41] H. -Y. Sun, H. -J. Sohn, O. Yamamoto, Y. Takeda, N. Imanishi, Enhanced lithium-ion transport in PEO-based composite polymer electrolytes with ferroelectric BaTiO3, J. Electrochem. Soc. 146 (1999) 1672–1676, https://doi.org/10.1149/1.1391824.
[42] Y. Inda, T. Katoh, M. Baba, Development of all-solid lithium-ion battery using Li-ion conducting glass-ceramics, J. Power Sources 174 (2007) 741–744, https://doi.org/10.1016/j.jpowsour.2007.06.234.
[43] J. Hassoun, B. Scrosati, Moving to a solid-state configuration: a valid approach to making lithium-sulfur batteries viable for practical applications, Adv. Mater. 22 (2010) 5198–5201, https://doi.org/10.1002/adma.201002584.
[44] L. Yang, D. Wei, M. Xu, Y. Yao, Q. Chen, Transferring lithium ions in nanochannels: a PEO/Li^+ solid polymer electrolyte design, Angew. Chem. Int. Ed. 53 (2014) 3631–3635, https://doi.org/10.1002/anie.201307423.
[45] W. Liu, N. Liu, J. Sun, P.-C. Hsu, Y. Li, H.-W. Lee, Y. Cui, Ionic conductivity enhancement of polymer electrolytes with ceramic nanowire fillers, Nano Lett. 15 (2015) 2740–2745, https://doi.org/10.1021/acs.nanolett.5b00600.
[46] S. Zekoll, C. Marriner-Edwards, A.K.O. Hekselman, J. Kasemchainan, C. Kuss, D.E.J. Armstrong, D. Cai, R.J. Wallace, F.H. Richter, J.H.J. Thijssen, P.G. Bruce, Hybrid electrolytes with 3D bicontinuous ordered ceramic and polymer microchannels for all-solid-state batteries, Energy Environ. Sci. 11 (2018) 185–201, https://doi.org/10.1039/C7EE02723K.
[47] J. Wan, J. Xie, X. Kong, Z. Liu, K. Liu, F. Shi, A. Pei, H. Chen, W. Chen, J. Chen, X. Zhang, L. Zong, J. Wang, L.-Q. Chen, J. Qin, Y. Cui, Ultrathin, flexible, solid polymer composite electrolyte enabled with aligned nanoporous host for lithium batteries, Nat. Nanotechnol. 14 (2019) 705–711, https://doi.org/10.1038/s41565-019-0465-3.
[48] H. Huo, B. Wu, T. Zhang, X. Zheng, L. Ge, T. Xu, X. Guo, X. Sun, Anion-immobilized polymer electrolyte achieved by cationic metal-organic framework filler for dendrite-free solid-state batteries, Energy Storage Mater. 18 (2019) 59–67, https://doi.org/10.1016/j.ensm.2019.01.007.
[49] H. Chen, D. Adekoya, L. Hencz, J. Ma, S. Chen, C. Yan, H. Zhao, G. Cui, S. Zhang, Stable seamless interfaces and rapid ionic conductivity of Ca–CeO_2/LiTFSI/PEO composite electrolyte for high-rate and high-voltage all-solid-state battery, Adv. Energy Mater. 10 (2020) 2000049, https://doi.org/10.1002/aenm.202000049.
[50] S. Xia, B. Yang, H. Zhang, J. Yang, W. Liu, S. Zheng, Ultrathin layered double hydroxide nanosheets enabling composite polymer electrolyte for all-solid-state lithium batteries at room temperature, Adv. Funct. Mater. 31 (2021) 2101168, https://doi.org/10.1002/adfm.202101168.
[51] L. Du, B. Zhang, W. Deng, Y. Cheng, L. Xu, L. Mai, Hierarchically self-assembled MOF network enables continuous ion transport and high mechanical strength, Adv. Energy Mater. 12 (2022) 2200501, https://doi.org/10.1002/aenm.202200501.
[52] Y. Jin, X. Zong, X. Zhang, Z. Jia, H. Xie, Y. Xiong, Constructing 3D Li^+-percolated transport network in composite polymer electrolytes for rechargeable quasi-solid-state lithium batteries, Energy Storage Mater. 49 (2022) 433–444, https://doi.org/10.1016/j.ensm.2022.04.035.
[53] P. Shi, J. Ma, M. Liu, S. Guo, Y. Huang, S. Wang, L. Zhang, L. Chen, K. Yang, X. Liu, Y. Li, X. An, D. Zhang, X. Cheng, Q. Li, W. Lv, G. Zhong, Y.-B. He, F. Kang, A dielectric electrolyte composite with high lithium-ion conductivity for high-voltage solid-state lithium metal batteries, Nat. Nanotechnol. 18 (2023) 602–610, https://doi.org/10.1038/s41565-023-01341-2.
[54] L.-Z. Fan, H. He, C.-W. Nan, Tailoring inorganic–polymer composites for the mass production of solid-state batteries, Nat. Rev. Mater. 6 (2021) 1003–1019, https://doi.org/10.1038/s41578-021-00320-0.
[55] V. Vijayakumar, M. Ghosh, K. Asokan, S.B. Sukumaran, S. Kurungot, J. Mindemark, D. Brandell, M. Winter, J.R. Nair, 2D layered nanomaterials as fillers in polymer composite electrolytes for lithium batteries, Adv. Energy Mater. 13 (2023) 2203326, https://doi.org/10.1002/aenm.202203326.
[56] L. Du, B. Zhang, X. Wang, C. Dong, L. Mai, L. Xu, 3D frameworks in composite polymer electrolytes: synthesis, mechanisms, and applications, Chem. Eng. J. 451 (2023) 138787, https://doi.org/10.1016/j.cej.2022.138787.
[57] Y. Liang, W. Lai, Z. Miao, S. Chou, Nanocomposite materials for the sodium–ion battery: a review, Small 14 (2018) 1702514, https://doi.org/10.1002/smll.201702514.

[58] J. Wan, J. Xie, D.G. Mackanic, W. Burke, Z. Bao, Y. Cui, Status, promises, and challenges of nanocomposite solid-state electrolytes for safe and high performance lithium batteries, Mater. Today Nano 4 (2018) 1–16, https://doi.org/10.1016/j.mtnano.2018.12.003.

[59] D.H.S. Tan, A. Banerjee, Z. Chen, Y.S. Meng, From nanoscale interface characterization to sustainable energy storage using all-solid-state batteries, Nat. Nanotechnol. 15 (2020) 170–180, https://doi.org/10.1038/s41565-020-0657-x.

[60] M.-C. Pang, K. Yang, R. Brugge, T. Zhang, X. Liu, F. Pan, S. Yang, A. Aguadero, B. Wu, M. Marinescu, H. Wang, G.J. Offer, Interactions are important: linking multi-physics mechanisms to the performance and degradation of solid-state batteries, Mater. Today 49 (2021) 145–183, https://doi.org/10.1016/j.mattod.2021.02.011.

[61] X. Yang, K.R. Adair, X. Gao, X. Sun, Recent advances and perspectives on thin electrolytes for high-energy-density solid-state lithium batteries, Energy Environ. Sci. 14 (2021) 643–671, https://doi.org/10.1039/D0EE02714F.

[62] Z. Zeng, J. Cheng, Y. Li, H. Zhang, D. Li, H. Liu, F. Ji, Q. Sun, L. Ci, Composite cathode for all-solid-state lithium batteries: progress and perspective, Mater. Today Phys. 32 (2023) 101009, https://doi.org/10.1016/j.mtphys.2023.101009.

[63] Q. Wang, P. Zou, L. Ren, S. Wang, Y. Wang, Z. Huang, Z. Hou, Z. Jiang, X. Lu, T. Lu, L. Guan, L. Hou, C. Yang, W. Liu, Y. Wei, Ultrathin composite Li electrode for high-performance Li metal batteries: a review from synthetic chemistry, Adv. Funct. Mater. 33 (2023) 2213648, https://doi.org/10.1002/adfm.202213648.

[64] C.-Z. Zhao, X.-Q. Zhang, X.-B. Cheng, R. Zhang, R. Xu, P.-Y. Chen, H.-J. Peng, J.-Q. Huang, Q. Zhang, An anion-immobilized composite electrolyte for dendrite-free lithium metal anodes, Proc. Natl. Acad. Sci. USA 114 (2017) 11069–11074, https://doi.org/10.1073/pnas.1708489114.

[65] N. Wu, P. Chien, Y. Qian, Y. Li, H. Xu, N.S. Grundish, B. Xu, H. Jin, Y. Hu, G. Yu, J.B. Goodenough, Enhanced surface interactions enable fast Li^+ conduction in oxide/polymer composite electrolyte, Angew. Chem. Int. Ed. 59 (2020) 4131–4137, https://doi.org/10.1002/anie.201914478.

[66] J. Lu, Y. Liu, P. Yao, Z. Ding, Q. Tang, J. Wu, Z. Ye, K. Huang, X. Liu, Hybridizing poly(vinylidene fluoride-co-hexafluoropropylene) with $Li_{6.5}La_3Zr_{1.5}Ta_{0.5}O_{12}$ as a lithium-ion electrolyte for solid state lithium metal batteries, Chem. Eng. J. 367 (2019) 230–238, https://doi.org/10.1016/j.cej.2019.02.148.

[67] D. Lin, W. Liu, Y. Liu, H.R. Lee, P.-C. Hsu, K. Liu, Y. Cui, High ionic conductivity of composite solid polymer electrolyte via in situ synthesis of monodispersed SiO_2 nanospheres in poly(ethylene oxide), Nano Lett. 16 (2016) 459–465, https://doi.org/10.1021/acs.nanolett.5b04117.

[68] C. Park, Electrochemical stability and conductivity enhancement of composite polymer electrolytes, Solid State Ion. 159 (2003) 111–119, https://doi.org/10.1016/S0167-2738(03)00025-0.

[69] C. Hu, Y. Shen, M. Shen, X. Liu, H. Chen, C. Liu, T. Kang, F. Jin, L. Li, J. Li, Y. Li, N. Zhao, X. Guo, W. Lu, B. Hu, L. Chen, Superionic conductors *via* bulk interfacial conduction, J. Am. Chem. Soc. 142 (2020) 18035–18041, https://doi.org/10.1021/jacs.0c07060.

[70] B. Jiang, F. Li, T. Hou, Y. Liu, H. Cheng, H. Wang, D. Li, H. Xu, Y. Huang, Polymer electrolytes shielded by 2D $Li_{0.46}Mn_{0.77}PS_3$ Li^+-conductors for all-solid-state lithium-metal batteries, Energy Storage Mater. 56 (2023) 183–191, https://doi.org/10.1016/j.ensm.2023.01.011.

[71] W. Liu, D. Lin, J. Sun, G. Zhou, Y. Cui, Improved lithium ionic conductivity in composite polymer electrolytes with oxide-ion conducting nanowires, ACS Nano 10 (2016) 11407–11413, https://doi.org/10.1021/acsnano.6b06797.

[72] Y. Li, L. Zhang, Z. Sun, G. Gao, S. Lu, M. Zhu, Y. Zhang, Z. Jia, C. Xiao, H. Bu, K. Xi, S. Ding, Hexagonal boron nitride induces anion trapping in a polyethylene oxide based solid polymer electrolyte for lithium dendrite inhibition, J. Mater. Chem. A 8 (2020) 9579–9589, https://doi.org/10.1039/D0TA03677C.

[73] M. Yao, Q. Ruan, Y. Wang, L. Du, Q. Li, L. Xu, R. Wang, H. Zhang, A robust dual-polymer@inorganic networks composite polymer electrolyte toward ultra-long-life and high-voltage Li/Li-rich metal battery, Adv. Funct. Mater. 33 (2023) 2213702, https://doi.org/10.1002/adfm.202213702.

[74] W. Dieterich, O. Dürr, P. Pendzig, A. Bunde, A. Nitzan, Percolation concepts in solid state ionics, Physica A 266 (1999) 229–237, https://doi.org/10.1016/S0378-4371(98)00597-4.

[75] J.A. Isaac, D. Devaux, R. Bouchet, Dense inorganic electrolyte particles as a lever to promote composite electrolyte conductivity, Nat. Mater. 21 (2022) 1412–1418, https://doi.org/10.1038/s41563-022-01343-w.

[76] Z. Li, H.-M. Huang, J.-K. Zhu, J.-F. Wu, H. Yang, L. Wei, X. Guo, Ionic conduction in composite polymer electrolytes: case of PEO:Ga-LLZO composites, ACS Appl. Mater. Interfaces 11 (2019) 784–791, https://doi.org/10.1021/acsami.8b17279.

[77] S. Lv, X. He, Z. Ji, S. Yang, L. Feng, X. Fu, W. Yang, Y. Wang, A supertough and highly-conductive nano-dipole doped composite polymer electrolyte with hybrid Li^+ -solvation microenvironment for lithium metal batteries, Adv. Energy Mater. 13 (2023) 2302711, https://doi.org/10.1002/aenm.202302711.

[78] L. Chen, W. Li, L. Fan, C. Nan, Q. Zhang, Intercalated electrolyte with high transference number for dendrite-free solid-state lithium batteries, Adv. Funct. Mater. 29 (2019) 1901047, https://doi.org/10.1002/adfm.201901047.

[79] Y. Gong, K. Fu, S. Xu, J. Dai, T.R. Hamann, L. Zhang, G.T. Hitz, Z. Fu, Z. Ma, D.W. McOwen, X. Han, L. Hu, E.D. Wachsman, Lithium-ion conductive ceramic textile: a new architecture for flexible solid-state lithium metal batteries, Mater. Today 21 (2018) 594–601, https://doi.org/10.1016/j.mattod.2018.01.001.

[80] Z. Gadjourova, D. Martín Y Marero, K.H. Andersen, Y.G. Andreev, P.G. Bruce, Structures of the polymer electrolyte complexes PEO_6: $LiXF_6$ (X = P, Sb), determined from neutron powder diffraction data, Chem. Mater. 13 (2001) 1282–1285, https://doi.org/10.1021/cm000949k.

[81] Z. Gadjourova, Y.G. Andreev, D.P. Tunstall, P.G. Bruce, Ionic conductivity in crystalline polymer electrolytes, Nature 412 (2001) 520–523, https://doi.org/10.1038/35087538.

[82] N. Wu, P.-H. Chien, Y. Li, A. Dolocan, H. Xu, B. Xu, N.S. Grundish, H. Jin, Y.-Y. Hu, J.B. Goodenough, Fast Li^+ conduction mechanism and interfacial chemistry of a NASICON/polymer composite electrolyte, J. Am. Chem. Soc. 142 (2020) 2497–2505, https://doi.org/10.1021/jacs.9b12233.

[83] M. Liu, S. Zhang, E.R.H. Van Eck, C. Wang, S. Ganapathy, M. Wagemaker, Improving Li-ion interfacial transport in hybrid solid electrolytes, Nat. Nanotechnol. 17 (2022) 959–967, https://doi.org/10.1038/s41565-022-01162-9.

[84] M. Armand, The history of polymer electrolytes, Solid State Ion. 69 (1994) 309–319, https://doi.org/10.1016/0167-2738(94)90419-7.

[85] S. Kalnaus, A.S. Sabau, W.E. Tenhaeff, N.J. Dudney, C. Daniel, Design of composite polymer electrolytes for Li ion batteries based on mechanical stability criteria, J. Power Sources 201 (2012) 280–287, https://doi.org/10.1016/j.jpowsour.2011.11.020.

[86] P. Johansson, M.A. Ratner, D.F. Shriver, The influence of inert oxide fillers on poly (ethylene oxide) and amorphous poly(ethylene oxide) based polymer electrolytes, J. Phys. Chem. B 105 (2001) 9016–9021, https://doi.org/10.1021/jp010868r.

[87] H. Xu, H. Zhang, J. Ma, G. Xu, T. Dong, J. Chen, G. Cui, Overcoming the challenges of 5 V spinel $LiNi_{0.5}$ $Mn_{1.5}O_4$ cathodes with solid polymer electrolytes, ACS Energy Lett. 4 (2019) 2871–2886, https://doi.org/10.1021/acsenergylett.9b01871.

[88] Y. Chen, Y. Cui, S. Wang, Y. Xiao, J. Niu, J. Huang, F. Wang, S. Chen, Durable and adjustable interfacial engineering of polymeric electrolytes for both stable Ni-rich cathodes and high-energy metal anodes, Adv. Mater. 35 (2023) 2300982, https://doi.org/10.1002/adma.202300982.

[89] J. Qiu, X. Liu, R. Chen, Q. Li, Y. Wang, P. Chen, L. Gan, S. Lee, D. Nordlund, Y. Liu, X. Yu, X. Bai, H. Li, L. Chen, Enabling stable cycling of 4.2 V high-voltage all-solid-state batteries with PEO-based solid electrolyte, Adv. Funct. Mater. 30 (2020) 1909392, https://doi.org/10.1002/adfm.201909392.

[90] X. Wang, Y. Song, X. Jiang, Q. Liu, J. Dong, J. Wang, X. Zhou, B. Li, G. Yin, Z. Jiang, J. Wang, Constructing interfacial nanolayer stabilizes 4.3 V high-voltage all-solid-state lithium batteries with PEO-based solid-state electrolyte, Adv. Funct. Mater. 32 (2022) 2113068, https://doi.org/10.1002/adfm.202113068.

[91] X. Yang, M. Jiang, X. Gao, D. Bao, Q. Sun, N. Holmes, H. Duan, S. Mukherjee, K. Adair, C. Zhao, J. Liang, W. Li, J. Li, Y. Liu, H. Huang, L. Zhang, S. Lu, Q. Lu, R. Li, C.V. Singh, X. Sun, Determining the limiting factor of the electrochemical stability window for PEO-based solid polymer electrolytes: main chain or terminal –OH group? Energy Environ. Sci. 13 (2020) 1318–1325, https://doi.org/10.1039/D0EE00342E.

[92] L. Li, H. Duan, J. Li, L. Zhang, Y. Deng, G. Chen, Toward high performance all-solid-state lithium batteries with high-voltage cathode materials: design strategies for solid electrolytes, cathode interfaces, and composite electrodes, Adv. Energy Mater. 11 (2021) 2003154, https://doi.org/10.1002/aenm.202003154.

[93] H. Chen, Q. Liu, M. Jing, F. Chen, W. Yuan, B. Ju, F. Tu, X. Shen, S. Qin, Improved interface stability and room-temperature performance of solid-state lithium batteries by integrating cathode/electrolyte and graphite coating, ACS Appl. Mater. Interfaces 12 (2020) 15120–15127, https://doi.org/10.1021/acsami.9b22690.

[94] M. Yao, Q. Ruan, S. Pan, H. Zhang, S. Zhang, An ultrathin asymmetric solid polymer electrolyte with intensified ion transport regulated by biomimetic channels enabling wide-temperature high-voltage lithium-metal battery, Adv. Energy Mater. 13 (2023) 2203640, https://doi.org/10.1002/aenm.202203640.

[95] X. Pan, H. Sun, Z. Wang, H. Huang, Q. Chang, J. Li, J. Gao, S. Wang, H. Xu, Y. Li, W. Zhou, High voltage stable polyoxalate catholyte with cathode coating for all-solid-state Li-metal/NMC622 batteries, Adv. Energy Mater. 10 (2020) 2002416, https://doi.org/10.1002/aenm.202002416.

[96] Y. Liu, X. An, K. Yang, J. Ma, J. Mi, D. Zhang, X. Cheng, Y. Li, Y. Ma, M. Liu, F. Kang, Y.-B. He, Achieving a high loading of cathode in PVDF-based solid-state battery, Energy Environ. Sci. 17 (2024) 344–353, https://doi.org/10.1039/D3EE03108J.

[97] S. Huo, L. Sheng, W. Xue, L. Wang, H. Xu, H. Zhang, B. Su, M. Lyu, X. He, Challenges of stable ion pathways in cathode electrode for all-solid-state lithium batteries: a review, Adv. Energy Mater. 13 (2023) 2204343, https://doi.org/10.1002/aenm.202204343.

[98] R. He, S. Lei, M. Liu, M. Qin, W. Zhong, S. Cheng, J. Xie, Enhanced dynamic phase stability and suppressed Mn dissolution in low-tortuosity spinel LMO electrode, Energy Mater. Adv. 2022 (2022) 0003, https://doi.org/10.34133/energymatadv.0004.

[99] L. Wang, J. Qiu, X. Wang, L. Chen, G. Cao, J. Wang, H. Zhang, X. He, Insights for understanding multiscale degradation of $LiFePO_4$ cathodes, eScience 2 (2022) 125–137, https://doi.org/10.1016/j.esci.2022.03.006.

[100] J. Pan, Y. Zhang, J. Wang, Z. Bai, R. Cao, N. Wang, S. Dou, F. Huang, A quasi-double-layer solid electrolyte with adjustable interphases enabling high-voltage solid-state batteries, Adv. Mater. 34 (2022) 2107183, https://doi.org/10.1002/adma.202107183.

[101] T. Deng, L. Cao, X. He, A.-M. Li, D. Li, J. Xu, S. Liu, P. Bai, T. Jin, L. Ma, M.A. Schroeder, X. Fan, C. Wang, In situ formation of polymer-inorganic solid-electrolyte interphase for stable polymeric solid-state lithium-metal batteries, Chem 7 (2021) 3052–3068, https://doi.org/10.1016/j.chempr.2021.06.019.

[102] H.-L. Guo, H. Sun, Z.-L. Jiang, J.-Y. Hu, C.-S. Luo, M.-Y. Gao, J.-Y. Cheng, W.-K. Shi, H.-J. Zhou, S.-G. Sun, Asymmetric structure design of electrolytes with flexibility and lithium dendrite-suppression ability for solid-state lithium batteries, ACS Appl. Mater. Interfaces 11 (2019) 46783–46791, https://doi.org/10.1021/acsami.9b16312.

[103] H. Zhai, T. Gong, B. Xu, Q. Cheng, D. Paley, B. Qie, T. Jin, Z. Fu, L. Tan, Y.-H. Lin, C.-W. Nan, Y. Yang, Stabilizing polyether electrolyte with a 4 V metal oxide cathode by nanoscale interfacial coating, ACS Appl. Mater. Interfaces 11 (2019) 28774–28780, https://doi.org/10.1021/acsami.9b04932.

[104] B. Xu, X. Li, C. Yang, Y. Li, N.S. Grundish, P.-H. Chien, K. Dong, I. Manke, R. Fang, N. Wu, H. Xu, A. Dolocan, J.B. Goodenough, Interfacial chemistry enables stable cycling of all-solid-state Li metal batteries at high current densities, J. Am. Chem. Soc. 143 (2021) 6542–6550, https://doi.org/10.1021/jacs.1c00752.

[105] Y. Lin, M. Wu, J. Sun, L. Zhang, Q. Jian, T. Zhao, A high-capacity, long-cycling all-solid-state lithium battery enabled by integrated cathode/ultrathin solid electrolyte, Adv. Energy Mater. 11 (2021) 2101612, https://doi.org/10.1002/aenm.202101612.
[106] S. Wang, Q. Sun, Q. Zhang, C. Li, C. Xu, Y. Ma, X. Shi, H. Zhang, D. Song, L. Zhang, Li-ion transfer mechanism of ambient-temperature solid polymer electrolyte toward lithium metal battery, Adv. Energy Mater. 13 (2023) 2204036, https://doi.org/10.1002/aenm.202204036.
[107] X. Hu, J. Yu, Y. Wang, W. Guo, X. Zhang, M. Armand, F. Kang, G. Wang, D. Zhou, B. Li, A lithium intrusion-blocking interfacial shield for wide-pressure-range solid-state lithium metal batteries, Adv. Mater. (2023) 2308275, https://doi.org/10.1002/adma.202308275.
[108] Q. Cheng, A. Li, N. Li, S. Li, A. Zangiabadi, T.-D. Li, W. Huang, A.C. Li, T. Jin, Q. Song, W. Xu, N. Ni, H. Zhai, M. Dontigny, K. Zaghib, X. Chuan, D. Su, K. Yan, Y. Yang, Stabilizing solid electrolyte-anode interface in Li-metal batteries by boron nitride-based nanocomposite coating, Joule 3 (2019) 1510–1522, https://doi.org/10.1016/j.joule.2019.03.022.
[109] A.E. Abdelmaoula, L. Du, L. Xu, Y. Cheng, A.A. Mahdy, M. Tahir, Z. Liu, L. Mai, Biomimetic brain-like nanostructures for solid polymer electrolytes with fast ion transport, Sci. China Mater. 65 (2022) 1476–1484, https://doi.org/10.1007/s40843-021-1940-2.
[110] J. Hu, C. Lai, K. Chen, Q. Wu, Y. Gu, C. Wu, C. Li, Dual fluorination of polymer electrolyte and conversion-type cathode for high-capacity all-solid-state lithium metal batteries, Nat. Commun. 13 (2022) 7914, https://doi.org/10.1038/s41467-022-35636-0.
[111] Q. Wu, M. Fang, S. Jiao, S. Li, S. Zhang, Z. Shen, S. Mao, J. Mao, J. Zhang, Y. Tan, K. Shen, J. Lv, W. Hu, Y. He, Y. Lu, Phase regulation enabling dense polymer-based composite electrolytes for solid-state lithium metal batteries, Nat. Commun. 14 (2023) 6296, https://doi.org/10.1038/s41467-023-41808-3.
[112] G. Yang, X. Bai, Y. Zhang, Z. Guo, C. Zhao, L. Fan, N. Zhang, A bridge between ceramics electrolyte and interface layer to fast Li^+ transfer for low interface impedance solid-state batteries, Adv. Funct. Mater. 33 (2023) 2211387, https://doi.org/10.1002/adfm.202211387.
[113] X. Zhang, J. Xie, F. Shi, D. Lin, Y. Liu, W. Liu, A. Pei, Y. Gong, H. Wang, K. Liu, Y. Xiang, Y. Cui, Vertically aligned and continuous nanoscale ceramic–polymer interfaces in composite solid polymer electrolytes for enhanced ionic conductivity, Nano Lett. 18 (2018) 3829–3838, https://doi.org/10.1021/acs.nanolett.8b01111.
[114] X. Li, L. Cong, S. Ma, S. Shi, Y. Li, S. Li, S. Chen, C. Zheng, L. Sun, Y. Liu, H. Xie, Low resistance and high stable solid–liquid electrolyte interphases enable high-voltage solid-state lithium metal batteries, Adv. Funct. Mater. 31 (2021) 2010611, https://doi.org/10.1002/adfm.202010611.
[115] T.T. Vu, H.J. Cheon, S.Y. Shin, G. Jeong, E. Wi, M. Chang, Hybrid electrolytes for solid-state lithium batteries: challenges, progress, and prospects, Energy Storage Mater. 61 (2023) 102876, https://doi.org/10.1016/j.ensm.2023.102876.
[116] Y. Hu, L. Li, H. Tu, X. Yi, J. Wang, J. Xu, W. Gong, H. Lin, X. Wu, M. Liu, Janus electrolyte with modified Li^+ solvation for high-performance solid-state lithium batteries, Adv. Funct. Mater. 32 (2022) 2203336, https://doi.org/10.1002/adfm.202203336.
[117] S. Guo, T. Wu, Y. Sun, S. Zhang, B. Li, H. Zhang, M. Qi, X. Liu, A. Cao, L. Wan, Interface engineering of a ceramic electrolyte by Ta_2O_5 nanofilms for ultrastable lithium metal batteries, Adv. Funct. Mater. 32 (2022) 2201498, https://doi.org/10.1002/adfm.202201498.
[118] Z. Shi, X. Zhang, W. Guo, QunJie Xu, Y. Min, Interfacial electric field effect of double-network composite electrolyte for ultra-stable lithium batteries, Chem. Eng. J. 440 (2022) 135779, https://doi.org/10.1016/j.cej.2022.135779.
[119] L. Liu, T. Wang, L. Sun, T. Song, H. Yan, C. Li, D. Mu, J. Zheng, Y. Dai, Stable cycling of all-solid-state lithium metal batteries enabled by salt engineering of PEO-based polymer electrolytes, Energy Environ. Mater. (2023) e12580, https://doi.org/10.1002/eem2.12580.
[120] Q. Cheng, T. Jin, Y. Miao, Z. Liu, J. Borovilas, H. Zhang, S. Liu, S.-Y. Kim, R. Zhang, H. Wang, X. Chen, L.-Q. Chen, J. Li, W. Min, Y. Yang, Stabilizing lithium plating in polymer electrolytes by concentration-polarization-induced phase transformation, Joule 6 (2022) 2372–2389, https://doi.org/10.1016/j.joule.2022.08.001.
[121] Q. Zhang, B. Yue, C. Shao, H. Shao, L. Li, X. Dong, J. Wang, W. Yu, Suppression of lithium dendrites in all-solid-state lithium batteries by using a Janus-structured composite solid electrolyte, Chem. Eng. J. 443 (2022) 136479, https://doi.org/10.1016/j.cej.2022.136479.
[122] L. Zhao, L. Du, H. Xu, J. Deng, L. Xu, Silicon layer on polymer electrolyte as a dendrite stopper for stable lithium metal batteries, ACS Appl. Energy Mater. 6 (2023) 9523–9531, https://doi.org/10.1021/acsaem.3c01498.
[123] M. Yao, Q. Ruan, T. Yu, H. Zhang, S. Zhang, Solid polymer electrolyte with in-situ generated fast Li^+ conducting network enable high voltage and dendrite-free lithium metal battery, Energy Storage Mater. 44 (2022) 93–103, https://doi.org/10.1016/j.ensm.2021.10.009.
[124] S. Zhang, F. Sun, X. Du, X. Zhang, L. Huang, J. Ma, S. Dong, A. Hilger, I. Manke, L. Li, B. Xie, J. Li, Z. Hu, A.C. Komarek, H.-J. Lin, C.-Y. Kuo, C.-T. Chen, P. Han, G. Xu, Z. Cui, G. Cui, *In situ* -polymerized lithium salt as a polymer electrolyte for high-safety lithium metal batteries, Energy Environ. Sci. 16 (2023) 2591–2602, https://doi.org/10.1039/D3EE00558E.
[125] H. Yang, B. Zhang, M. Jing, X. Shen, L. Wang, H. Xu, X. Yan, X. He, In situ catalytic polymerization of a highly homogeneous PDOL composite electrolyte for long-cycle high-voltage solid-state lithium batteries, Adv. Energy Mater. 12 (2022) 2201762, https://doi.org/10.1002/aenm.202201762.
[126] P. Johansson, P. Jacobsson, TiO_2 nano-particles in polymer electrolytes: surface interactions, Solid State Ion. 170 (2004) 73–78, https://doi.org/10.1016/j.ssi.2003.10.012.
[127] R. Fang, Y. Li, N. Wu, B. Xu, Y. Liu, A. Manthiram, J.B. Goodenough, Ultra-thin single-particle-layer sodium beta-alumina-based composite polymer electrolyte membrane for sodium-metal batteries, Adv. Funct. Mater. 33 (2023) 2211229, https://doi.org/10.1002/adfm.202211229.
[128] X. Wang, C. Fu, Z. Feng, H. Huo, X. Yin, G. Gao, G. Yin, L. Ci, Y. Tong, Z. Jiang, J. Wang, Flyash/polymer composite electrolyte with internal binding interaction enables highly-stable extrinsic-interfaces of all-solid-state lithium batteries, Chem. Eng. J. 428 (2022) 131041, https://doi.org/10.1016/j.cej.2021.131041.
[129] O. Sheng, C. Jin, J. Luo, H. Yuan, H. Huang, Y. Gan, J. Zhang, Y. Xia, C. Liang, W. Zhang, X. Tao, $Mg_2B_2O_5$ nanowire enabled multifunctional solid-state electrolytes with high ionic conductivity, excellent mechanical properties, and flame-retardant performance, Nano Lett. 18 (2018) 3104–3112, https://doi.org/10.1021/acs.nanolett.8b00659.
[130] Q. Wang, J.-F. Wu, Z.-Y. Yu, X. Guo, Composite polymer electrolytes reinforced by two-dimensional layer-double-hydroxide nanosheets for dendrite-free lithium batteries, Solid State Ion. 347 (2020) 115275, https://doi.org/10.1016/j.ssi.2020.115275.
[131] D. Lin, P.Y. Yuen, Y. Liu, W. Liu, N. Liu, R.H. Dauskardt, Y. Cui, A silica-aerogel-reinforced composite polymer electrolyte with high ionic conductivity and high modulus, Adv. Mater. 30 (2018) 1802661, https://doi.org/10.1002/adma.201802661.
[132] H. Liu, L. Xu, H. Tu, Z. Luo, F. Zhu, W. Deng, G. Zou, H. Hou, X. Ji, Interfacial interaction of multifunctional GQDs reinforcing polymer electrolytes for all-solid-state Li battery, Small 19 (2023) 2301275, https://doi.org/10.1002/smll.202301275.
[133] J.H. Park, K. Suh, Md.R. Rohman, W. Hwang, M. Yoon, K. Kim, Solid lithium electrolytes based on an organic molecular porous solid, Chem. Commun. 51 (2015) 9313–9316, https://doi.org/10.1039/C5CC02581H.
[134] H. Wang, Q. Wang, X. Cao, Y. He, K. Wu, J. Yang, H. Zhou, W. Liu, X. Sun, Thiol-branched solid polymer electrolyte featuring high strength, toughness, and lithium ionic conductivity for lithium-metal batteries, Adv. Mater. 32 (2020) 2001259, https://doi.org/10.1002/adma.202001259.
[135] Z. Lei, J. Shen, J. Wang, Q. Qiu, G. Zhang, S.-S. Chi, H. Xu, S. Li, W. Zhang, Y. Zhao, Y. Deng, C. Wang, Composite polymer electrolytes with uniform distribution of ionic liquid-grafted ZIF-90 nanofillers for high-performance solid-state Li batteries, Chem. Eng. J. 412 (2021) 128733, https://doi.org/10.1016/j.cej.2021.128733.
[136] X.-L. Zhang, F.-Y. Shen, X. Long, S. Zheng, Z. Ruan, Y.-P. Cai, X.-J. Hong, Q. Zheng, Fast Li^+ transport and superior interfacial chemistry within composite polymer electrolyte enables ultra-long cycling solid-state Li-metal batteries, Energy Storage Mater. 52 (2022) 201–209, https://doi.org/10.1016/j.ensm.2022.07.045.
[137] Y. Jiang, C. Xu, K. Xu, S. Li, J. Ni, Y. Wang, Y. Liu, J. Cai, C. Lai, Surface modification and structure constructing for improving the lithium ion transport properties of PVDF based solid electrolytes, Chem. Eng. J. 442 (2022) 136245, https://doi.org/10.1016/j.cej.2022.136245.
[138] J. Zhou, X. Wang, J. Fu, L. Chen, X. Wei, R. Jia, L. Shi, A 3D cross-linked metal-organic framework (MOF)-derived polymer electrolyte for dendrite-free solid-state lithium-ion batteries, Small (2023) 2309317, https://doi.org/10.1002/smll.202309317.
[139] X. Zhang, H. Zhang, Y. Geng, Z. Shi, S. Zhu, Q. Xu, Y. Min, A multifunctional nano filler for solid polymer electrolyte toward stable cycling for lithium-metal anodes in lithium–sulfur batteries, Chem. Eng. J. 444 (2022) 136328, https://doi.org/10.1016/j.cej.2022.136328.
[140] J. Kang, N. Deng, D. Shi, Y. Feng, Z. Wang, L. Gao, Y. Song, Y. Zhao, B. Cheng, G. Li, W. Kang, K. Zhang, Heterojunction-accelerating lithium salt dissociation in polymer solid electrolytes, Adv. Funct. Mater. 33 (2023) 2307263, https://doi.org/10.1002/adfm.202307263.
[141] B. Luo, W. Wang, Q. Wang, W. Ji, G. Yu, Z. Liu, Z. Zhao, X. Wang, S. Wang, J. Zhang, Facilitating ionic conductivity and interfacial stability via oxygen vacancies-enriched TiO_2 microrods for composite polymer electrolytes, Chem. Eng. J. 460 (2023) 141329, https://doi.org/10.1016/j.cej.2023.141329.
[142] T. Deng, Q. Han, J. Liu, C. Yang, J. Wang, M. Wang, Z. Wang, B. Zhou, Vertically aligned hollow mesoporous silica rods enabling composite polymer electrolytes with fast ionic conduction for lithium metal batteries, Adv. Funct. Mater. (2023) 2311952, https://doi.org/10.1002/adfm.202311952.
[143] F. He, Z. Hu, W. Tang, A. Wang, B. Wen, L. Zhang, J. Luo, Vertically hetero-structured solid electrolytes for lithium metal batteries, Adv. Funct. Mater. 32 (2022) 2201465, https://doi.org/10.1002/adfm.202201465.
[144] Q. Ma, S. Fu, A. Wu, Q. Deng, W. Li, D. Yue, B. Zhang, X. Wu, Z. Wang, Y. Guo, Designing bidirectionally functional polymer electrolytes for stable solid lithium metal batteries, Adv. Energy Mater. 13 (2023) 2203892, https://doi.org/10.1002/aenm.202203892.
[145] D.A. Vazquez-Molina, G.S. Mohammad-Pour, C. Lee, M.W. Logan, X. Duan, J.K. Harper, F.J. Uribe-Romo, Mechanically shaped two-dimensional covalent organic frameworks reveal crystallographic alignment and fast Li-ion conductivity, J. Am. Chem. Soc. 138 (2016) 9767–9770, https://doi.org/10.1021/jacs.6b05568.
[146] L. Wang, S. Yi, Q. Liu, Y. Li, Y. Hu, H. Tu, Y. Wang, A. Sun, F. Zhu, F. Mushtaq, B. Liu, P. Xue, W. Li, M. Liu, Bifunctional lithium-montmorillonite enabling solid electrolyte with superhigh ionic conductivity for high-performanced lithium metal batteries, Energy Storage Mater. 63 (2023) 102961, https://doi.org/10.1016/j.ensm.2023.102961.
[147] W. Liu, G. Li, W. Yu, L. Gao, D. Shi, J. Ju, N. Deng, W. Kang, Asymmetric organic-inorganic bi-functional composite solid-state electrolyte for long stable cycling of

high-voltage lithium battery, Energy Storage Mater. 63 (2023) 103005, https://doi.org/10.1016/j.ensm.2023.103005.
[148] Md.M. Hassan, A.A. Bristi, X. He, M. Trifkovic, G. Bobrov, Q. Lu, Novel nanoarchitecture of 3D ion transfer channel containing nanocomposite solid polymer electrolyte membrane based on holey graphene oxide and chitosan biopolymer, Chem. Eng. J. 466 (2023) 143159, https://doi.org/10.1016/j.cej.2023.143159.
[149] L. Yang, Q. Liu, H. Ma, Q. An, X. Wang, Y. Ding, Z. Mei, X. Sheng, L. Duan, J. Xie, H. Guo, Functional nanosheet fillers with fast Li^+ conduction for advanced all-solid-state lithium battery, Energy Storage Mater. 62 (2023) 102954, https://doi.org/10.1016/j.ensm.2023.102954.
[150] H. Lian, R. Momen, Y. Xiao, B. Song, X. Hu, F. Zhu, H. Liu, L. Xu, W. Deng, H. Hou, G. Zou, X. Ji, High ionic conductivity motivated by multiple ion-transport channels in 2D MOF-based lithium solid state battery, Adv. Funct. Mater. 33 (2023) 2306060, https://doi.org/10.1002/adfm.202306060.
[151] H. Jiang, Y. Du, X. Liu, J. Kong, M. Huang, P. Liu, T. Zhou, Composite polymer electrolytes incorporating two-dimensional metal–organic frameworks for ultra-long cycling in solid-state lithium batteries, J. Mater. Chem. A 11 (2023) 22371–22383, https://doi.org/10.1039/D3TA04074G.
[152] Y.M. Jeon, S. Kim, M. Lee, W.B. Lee, J.H. Park, Polymer-clay nanocomposite solid-state electrolyte with selective cation transport boosting and retarded lithium dendrite formation, Adv. Energy Mater. 10 (2020) 2003114, https://doi.org/10.1002/aenm.202003114.
[153] W. Tang, S. Tang, C. Zhang, Q. Ma, Q. Xiang, Y. Yang, J. Luo, Simultaneously enhancing the thermal stability, mechanical modulus, and electrochemical performance of solid polymer electrolytes by incorporating 2D sheets, Adv. Energy Mater. 8 (2018) 1800866, https://doi.org/10.1002/aenm.201800866.
[154] Q. Zhu, X. Wang, R. Clowes, P. Cui, L. Chen, M.A. Little, A.I. Cooper, 3D cage COFs: a dynamic three-dimensional covalent organic framework with high-connectivity organic cage nodes, J. Am. Chem. Soc. 142 (2020) 16842–16848, https://doi.org/10.1021/jacs.0c07732.
[155] Y. Xia, Q. Wang, Y. Liu, J. Zhang, X. Xia, H. Huang, Y. Gan, X. He, Z. Xiao, W. Zhang, Three-dimensional polyimide nanofiber framework reinforced polymer electrolyte for all-solid-state lithium metal battery, J. Colloid Interface Sci. 638 (2023) 908–917, https://doi.org/10.1016/j.jcis.2023.01.138.
[156] C. Li, L. Ou, Y. Liu, L. Xu, S. Zhou, L. Guo, H. Liu, Z. Zhang, M. Cui, G. Chen, J. Huang, J. Tao, A cellulose/polyethylene oxide gel polymer electrolyte with enhanced mechanical strength and high ionic conductivity for lithium-ion batteries, Adv. Mater. Technol. 8 (2023) 2202002, https://doi.org/10.1002/admt.202202002.
[157] H.-M. Wang, Z.-Y. Wang, C. Zhou, G.-R. Li, S. Liu, X.-P. Gao, A gel polymer electrolyte with Al_2O_3 nanofibers skeleton for lithium-sulfur batteries, Sci. China Mater. 66 (2023) 913–922, https://doi.org/10.1007/s40843-022-2252-1.
[158] X. Zhang, Q. Su, G. Du, B. Xu, S. Wang, Z. Chen, L. Wang, W. Huang, H. Pang, Stabilizing solid-state lithium metal batteries through in situ generated Janus-heterarchical LiF-rich SEI in ionic liquid confined 3D MOF/polymer membranes, Angew. Chem. Int. Ed. 62 (2023) e202304947, https://doi.org/10.1002/anie.202304947.
[159] G. Wang, Y. Liang, H. Liu, C. Wang, D. Li, L. Fan, Scalable, thin asymmetric composite solid electrolyte for high-performance all-solid-state lithium metal batteries, Interdiscip. Mater. 1 (2022) 434–444, https://doi.org/10.1002/idm2.12045.
[160] F. He, W. Tang, X. Zhang, L. Deng, J. Luo, High energy density solid state lithium metal batteries enabled by sub-5 μm solid polymer electrolytes, Adv. Mater. 33 (2021) 2105329, https://doi.org/10.1002/adma.202105329.
[161] J. Zhu, S. He, H. Tian, Y. Hu, C. Xin, X. Xie, L. Zhang, J. Gao, S. Hao, W. Zhou, L. Zhang, The influences of DMF content in composite polymer electrolytes on Li^+-conductivity and interfacial stability with Li-metal, Adv. Funct. Mater. 33 (2023) 2301165, https://doi.org/10.1002/adfm.202301165.
[162] J. Gou, Z. Zhang, S. Wang, J. Huang, K. Cui, H. Wang, An ultrahigh modulus gel electrolytes reforming the growing pattern of Li dendrites for interfacially stable lithium-metal batteries, Adv. Mater. (2023) 2309677, https://doi.org/10.1002/adma.202309677.
[163] X. Zhang, T. Liu, S. Zhang, X. Huang, B. Xu, Y. Lin, B. Xu, L. Li, C.-W. Nan, Y. Shen, Synergistic coupling between $Li_{6.75}La_3Zr_{1.75}Ta_{0.25}O_{12}$ and poly(vinylidene fluoride) induces high ionic conductivity, mechanical strength, and thermal stability of solid composite electrolytes, J. Am. Chem. Soc. 139 (2017) 13779–13785, https://doi.org/10.1021/jacs.7b06364.
[164] W. Liu, S.W. Lee, D. Lin, F. Shi, S. Wang, A.D. Sendek, Y. Cui, Enhancing ionic conductivity in composite polymer electrolytes with well-aligned ceramic nanowires, Nat. Energy 2 (2017) 17035, https://doi.org/10.1038/nenergy.2017.35.
[165] C. Wang, Y. Yang, X. Liu, H. Zhong, H. Xu, Z. Xu, H. Shao, F. Ding, Suppression of lithium dendrite formation by using LAGP-PEO (LiTFSI) composite solid electrolyte and lithium metal anode modified by PEO (LiTFSI) in all-solid-state lithium batteries, ACS Appl. Mater. Interfaces 9 (2017) 13694–13702, https://doi.org/10.1021/acsami.7b00336.
[166] H. Zhai, P. Xu, M. Ning, Q. Cheng, J. Mandal, Y. Yang, A flexible solid composite electrolyte with vertically aligned and connected ion-conducting nanoparticles for lithium batteries, Nano Lett. 17 (2017) 3182–3187, https://doi.org/10.1021/acs.nanolett.7b00715.
[167] A. Li, X. Liao, H. Zhang, L. Shi, P. Wang, Q. Cheng, J. Borovilas, Z. Li, W. Huang, Z. Fu, M. Dontigny, K. Zaghib, K. Myers, X. Chuan, X. Chen, Y. Yang, Nacre-inspired composite electrolytes for load-bearing solid-state lithium-metal batteries, Adv. Mater. 32 (2020) 1905517, https://doi.org/10.1002/adma.201905517.
[168] S. Song, Y. Wu, W. Tang, F. Deng, J. Yao, Z. Liu, R. Hu, Alamusi, Z. Wen, L. Lu, N. Hu, Composite solid polymer electrolyte with garnet nanosheets in poly (ethylene oxide), ACS Sustain. Chem. Eng. 7 (2019) 7163–7170, https://doi.org/10.1021/acssuschemeng.9b00143.
[169] J. Cheng, Y. Guo, H. Zhang, F. Ji, X. Zhou, Z. Zeng, H. Liu, Q. Sun, D. Li, L. Ci, 2D flake-like garnet electrolytes for solid-state lithium metal batteries, Chem. Eng. J. 479 (2024) 147244, https://doi.org/10.1016/j.cej.2023.147244.
[170] R. Lv, W. Kou, S. Guo, W. Wu, Y. Zhang, Y. Wang, J. Wang, Preparing two-dimensional ordered $Li_{0.33}La_{0.557}TiO_3$ crystal in interlayer channel of thin laminar inorganic solid-state electrolyte towards ultrafast Li^+ transfer, Angew. Chem. Int. Ed. 61 (2022) e202114220, https://doi.org/10.1002/anie.202114220.
[171] H. Xie, C. Yang, K. (Kelvin) Fu, Y. Yao, F. Jiang, E. Hitz, B. Liu, S. Wang, L. Hu, Flexible, scalable, and highly conductive garnet-polymer solid electrolyte templated by bacterial cellulose, Adv. Energy Mater. 8 (2018) 1703474, https://doi.org/10.1002/aenm.201703474.
[172] R. Sahore, B.L. Armstrong, X. Tang, C. Liu, K. Owensby, S. Kalnaus, X.C. Chen, Role of scaffold architecture and excess surface polymer layers in a 3D-interconnected ceramic/polymer composite electrolyte, Adv. Energy Mater. 13 (2023) 2203663, https://doi.org/10.1002/aenm.202203663.
[173] M.J. Palmer, S. Kalnaus, M.B. Dixit, A.S. Westover, K.B. Hatzell, N.J. Dudney, X.C. Chen, A three-dimensional interconnected polymer/ceramic composite as a thin film solid electrolyte, Energy Storage Mater. 26 (2020) 242–249, https://doi.org/10.1016/j.ensm.2019.12.031.
[174] Z. Zhang, Ying Huang, G. Zhang, L. Chao, Three–dimensional fiber network reinforced polymer electrolyte for dendrite–free all–solid–state lithium metal batteries, Energy Storage Mater. 41 (2021) 631–641, https://doi.org/10.1016/j.ensm.2021.06.030.
[175] P. Pan, M. Zhang, Z. Cheng, L. Jiang, J. Mao, C. Ni, Q. Chen, Y. Zeng, Y. Hu, K. (Kelvin) Fu, Garnet ceramic fabric-reinforced flexible composite solid electrolyte derived from silk template for safe and long-term stable all-solid-state lithium metal batteries, Energy Storage Mater. 47 (2022) 279–287, https://doi.org/10.1016/j.ensm.2022.02.018.
[176] Z. Li, W.-X. Sha, X. Guo, Three-dimensional garnet framework-reinforced solid composite electrolytes with high lithium-ion conductivity and excellent stability, ACS Appl. Mater. Interfaces 11 (2019) 26920–26927, https://doi.org/10.1021/acsami.9b07830.
[177] G. Wang, H. Liu, Y. Liang, C. Wang, L.-Z. Fan, Composite polymer electrolyte with three-dimensional ion transport channels constructed by NaCl template for solid-state lithium metal batteries, Energy Storage Mater. 45 (2022) 1212–1219, https://doi.org/10.1016/j.ensm.2021.11.021.
[178] Y. Zhao, J. Yan, W. Cai, Y. Lai, J. Song, J. Yu, B. Ding, Elastic and well-aligned ceramic LLZO nanofiber based electrolytes for solid-state lithium batteries, Energy Storage Mater. 23 (2019) 306–313, https://doi.org/10.1016/j.ensm.2019.04.043.
[179] K. Yu, H. Zeng, J. Ma, Y. Jiang, H. Li, L. Zhang, Q. Zhang, X. Shan, T. Li, X. Wu, H. Xu, W. Huang, C. Wang, S.-S. Chi, J. Wang, Q. Gong, Y. Deng, High-performance lithium metal batteries enabled by a nano-sized garnet solid-state electrolyte modified separator, Chem. Eng. J. 480 (2024) 148038, https://doi.org/10.1016/j.cej.2023.148038.
[180] Y. Zhang, L. Zhang, P. Guo, C. Zhang, X. Ren, Z. Jiang, J. Song, C. Shi, Porous garnet as filler of solid polymer electrolytes to enhance the performance of solid-state lithium batteries, Nano Res. (2023), https://doi.org/10.1007/s12274-023-6065-4.
[181] S.K. Fullerton-Shirey, J.K. Maranas, Effect of $LiClO_4$ on the structure and mobility of PEO-based solid polymer electrolytes, Macromolecules 42 (2009) 2142–2156, https://doi.org/10.1021/ma802502u.
[182] A. Manuel Stephan, K.S. Nahm, Review on composite polymer electrolytes for lithium batteries, Polymer 47 (2006) 5952–5964, https://doi.org/10.1016/j.polymer.2006.05.069.
[183] X. Zhang, J. Wang, D. Hu, W. Du, C. Hou, H. Jiang, Y. Wei, X. Liu, F. Jiang, J. Sun, H. Yuan, X. Huang, High-performance lithium metal batteries based on composite solid-state electrolytes with high ceramic content, Energy Storage Mater. 65 (2024) 103089, https://doi.org/10.1016/j.ensm.2023.103089.
[184] D.Y. Oh, Y.J. Nam, K.H. Park, S.H. Jung, S. Cho, Y.K. Kim, Y. Lee, S. Lee, Y.S. Jung, Excellent compatibility of solvate ionic liquids with sulfide solid electrolytes: toward favorable ionic contacts in bulk-type all-solid-state lithium-ion batteries, Adv. Energy Mater. 5 (2015) 1500865, https://doi.org/10.1002/aenm.201500865.
[185] H. Huo, M. Jiang, B. Mogwitz, J. Sann, Y. Yusim, T. Zuo, Y. Moryson, P. Minnmann, F.H. Richter, C. Veer Singh, J. Janek, Interface design enabling stable polymer/thiophosphate electrolyte separators for dendrite-free lithium metal batteries, Angew. Chem. Int. Ed. 62 (2023) e202218044, https://doi.org/10.1002/anie.202218044.
[186] W. Bao, Y. Zhang, L. Cao, Y. Jiang, H. Zhang, N. Zhang, Y. Liu, P. Yan, X. Wang, Y. Liu, H. Li, Y. Zhao, J. Xie, An H_2 O-initiated crosslinking strategy for ultrafine-nanoclusters-reinforced high-toughness polymer-in-plasticizer solid electrolyte, Adv. Mater. 35 (2023) 2304712, https://doi.org/10.1002/adma.202304712.
[187] W. Zhang, V. Koverga, S. Liu, J. Zhou, J. Wang, P. Bai, S. Tan, N.K. Dandu, Z. Wang, F. Chen, J. Xia, H. Wan, X. Zhang, H. Yang, B.L. Lucht, A.-M. Li, X.-Q. Yang, E. Hu, S.R. Raghavan, A.T. Ngo, C. Wang, Single-phase local-high-concentration solid polymer electrolytes for lithium-metal batteries, Nat. Energy (2024), https://doi.org/10.1038/s41560-023-01443-0.
[188] J. Zhang, N. Zhao, M. Zhang, Y. Li, P.K. Chu, X. Guo, Z. Di, X. Wang, H. Li, Flexible and ion-conducting membrane electrolytes for solid-state lithium batteries: dispersion of garnet nanoparticles in insulating polyethylene oxide, Nano Energy 28 (2016) 447–454, https://doi.org/10.1016/j.nanoen.2016.09.002.
[189] Y. Sun, X. Zhan, J. Hu, Y. Wang, S. Gao, Y. Shen, Y.-T. Cheng, Improving ionic conductivity with bimodal-sized $Li_7La_3Zr_2O_{12}$ fillers for composite polymer

electrolytes, ACS Appl. Mater. Interfaces 11 (2019) 12467–12475, https://doi.org/10.1021/acsami.8b21770.
[190] L. Chen, Y. Li, S.-P. Li, L.-Z. Fan, C.-W. Nan, J.B. Goodenough, PEO/garnet composite electrolytes for solid-state lithium batteries: from "ceramic-in-polymer" to "polymer-in-ceramic, Nano Energy 46 (2018) 176–184, https://doi.org/10.1016/j.nanoen.2017.12.037.
[191] H. Huo, Y. Chen, J. Luo, X. Yang, X. Guo, X. Sun, Rational design of hierarchical "ceramic-in-polymer" and "polymer-in-ceramic" electrolytes for dendrite-free solid-state batteries, Adv. Energy Mater. 9 (2019) 1804004, https://doi.org/10.1002/aenm.201804004.
[192] H. Duan, M. Fan, W. Chen, J. Li, P. Wang, W. Wang, J. Shi, Y. Yin, L. Wan, Y. Guo, Extended electrochemical window of solid electrolytes via heterogeneous multilayered structure for high-voltage lithium metal batteries, Adv. Mater. 31 (2019) 1807789, https://doi.org/10.1002/adma.201807789.
[193] J. Zheng, Y.-Y. Hu, New insights into the compositional dependence of Li-ion transport in polymer–ceramic composite electrolytes, ACS Appl. Mater. Interfaces 10 (2018) 4113–4120, https://doi.org/10.1021/acsami.7b17301.
[194] Y. Wang, L. Wu, Z. Lin, M. Tang, P. Ding, X. Guo, Z. Zhang, S. Liu, B. Wang, X. Yin, Z. Chen, K. Amine, H. Yu, Hydrogen bonds enhanced composite polymer electrolyte for high-voltage cathode of solid-state lithium battery, Nano Energy 96 (2022) 107105, https://doi.org/10.1016/j.nanoen.2022.107105.
[195] M. Cui, P.S. Lee, Solid polymer electrolyte with high ionic conductivity via layer-by-layer deposition, Chem. Mater. 28 (2016) 2934–2940, https://doi.org/10.1021/acs.chemmater.5b04739.
[196] L. Gao, N. Wu, N. Deng, Z. Li, J. Li, Y. Che, B. Cheng, W. Kang, R. Liu, Y. Li, Optimized CeO_2 nanowires with rich surface oxygen vacancies enable fast Li-ion conduction in composite polymer electrolytes, Energy Environ. Mater. 6 (2023) e12272, https://doi.org/10.1002/eem2.12272.
[197] Z. Zhang, Y. Huang, H. Gao, C. Li, J. Hang, P. Liu, MOF-derived multifunctional filler reinforced polymer electrolyte for solid-state lithium batteries, J. Energy Chem. 60 (2021) 259–271, https://doi.org/10.1016/j.jechem.2021.01.013.
[198] J. Yin, X. Xu, S. Jiang, H. Wu, L. Wei, Y. Li, J. He, K. Xi, Y. Gao, High ionic conductivity PEO-based electrolyte with 3D framework for dendrite-free solid-state lithium metal batteries at ambient temperature, Chem. Eng. J. 431 (2022) 133352, https://doi.org/10.1016/j.cej.2021.133352.
[199] Q. Xu, S. Tao, Q. Jiang, D. Jiang, Ion conduction in polyelectrolyte covalent organic frameworks, J. Am. Chem. Soc. 140 (2018) 7429–7432, https://doi.org/10.1021/jacs.8b03814.
[200] Y. Hu, N. Dunlap, S. Wan, S. Lu, S. Huang, I. Sellinger, M. Ortiz, Y. Jin, S. Lee, W. Zhang, Crystalline lithium imidazolate covalent organic frameworks with high Li-ion conductivity, J. Am. Chem. Soc. 141 (2019) 7518–7525, https://doi.org/10.1021/jacs.9b02448.
[201] Y. Wang, K. Zhang, X. Jiang, Z. Liu, S. Bian, Y. Pan, Z. Shan, M. Wu, B. Xu, G. Zhang, Branched poly(ethylene glycol)-functionalized covalent organic frameworks as solid electrolytes, ACS Appl. Energy Mater. 4 (2021) 11720–11725, https://doi.org/10.1021/acsaem.1c02426.
[202] T. Hamann, L. Zhang, Y. Gong, G. Godbey, J. Gritton, D. McOwen, G. Hitz, E. Wachsman, The effects of constriction factor and geometric tortuosity on Li-ion transport in porous solid-state Li-ion electrolytes, Adv. Funct. Mater. 30 (2020) 1910362, https://doi.org/10.1002/adfm.201910362.
[203] Y. Lu, S.K. Das, S.S. Moganty, L.A. Archer, Ionic liquid-nanoparticle hybrid electrolytes and their application in secondary lithium-metal batteries, Adv. Mater. 24 (2012) 4430–4435, https://doi.org/10.1002/adma.201201953.
[204] L. Gao, S. Luo, J. Li, B. Cheng, W. Kang, N. Deng, Core-shell structure nanofibers-ceramic nanowires based composite electrolytes with high Li transference number for high-performance all-solid-state lithium metal batteries, Energy Storage Mater. 43 (2021) 266–274, https://doi.org/10.1016/j.ensm.2021.09.013.
[205] P. Zhai, Z. Yang, Y. Wei, X. Guo, Y. Gong, Two-dimensional fluorinated graphene reinforced solid polymer electrolytes for high-performance solid-state lithium batteries, Adv. Energy Mater. 12 (2022) 2200967, https://doi.org/10.1002/aenm.202200967.
[206] Q. Ruan, M. Yao, J. Lu, Y. Wang, J. Kong, H. Zhang, S. Zhang, Mortise-tenon joints reinforced Janus composite solid-state electrolyte with fast kinetics for high-voltage lithium metal battery, Energy Storage Mater. 54 (2023) 294–303, https://doi.org/10.1016/j.ensm.2022.10.037.
[207] Y. Zheng, C. Wang, R. Zhang, S. Dai, H. Xie, J. Cui, X. Fang, Crosslinked polymer electrolyte constructed by metal-oxo clusters for solid lithium metal batteries, Energy Storage Mater. 57 (2023) 540–548, https://doi.org/10.1016/j.ensm.2023.02.037.
[208] S. Luo, N. Deng, H. Wang, Q. Zeng, Y. Li, W. Kang, B. Cheng, Facilitating Li^+ conduction channels and suppressing lithium dendrites by introducing Zn-based MOFs in composite electrolyte membrane with excellent thermal stability for solid-state lithium metal batteries, Chem. Eng. J. 474 (2023) 145683, https://doi.org/10.1016/j.cej.2023.145683.
[209] L. Huang, H. Fu, J. Duan, T. Wang, X. Zheng, Y. Huang, T. Zhao, Q. Yu, J. Wen, Y. Chen, D. Sun, W. Luo, Y. Huang, Negating Li^+ transfer barrier at solid-liquid electrolyte interface in hybrid batteries, Chem 8 (2022) 1928–1943, https://doi.org/10.1016/j.chempr.2022.03.002.
[210] J. Shim, H.J. Kim, B.G. Kim, Y.S. Kim, D.-G. Kim, J.-C. Lee, 2D boron nitride nanoflakes as a multifunctional additive in gel polymer electrolytes for safe, long cycle life and high rate lithium metal batteries, Energy Environ. Sci. 10 (2017) 1911–1916, https://doi.org/10.1039/C7EE01095H.
[211] J. Pan, H. Peng, Y. Yan, Y. Bai, J. Yang, N. Wang, S. Dou, F. Huang, Solid-state batteries designed with high ion conductive composite polymer electrolyte and silicon anode, Energy Storage Mater. 43 (2021) 165–171, https://doi.org/10.1016/j.ensm.2021.09.001.
[212] J. Luo, Q. Sun, J. Liang, K. Adair, F. Zhao, S. Deng, Y. Zhao, R. Li, H. Huang, R. Yang, S. Zhao, J. Wang, X. Sun, Rapidly in situ cross-linked poly(butylene oxide) electrolyte interface enabling halide-based all-solid-state lithium metal batteries, ACS Energy Lett. 8 (2023) 3676–3684, https://doi.org/10.1021/acsenergylett.3c01157.
[213] Y. Jing, Q. Lv, B. Wang, B. Wu, C. Li, S. Yang, D. Wang, H. Liu, S. Dou, High-performance intercalated composite solid electrolytes for lithium metal battery, Energy Storage Mater. 65 (2024) 103109, https://doi.org/10.1016/j.ensm.2023.103109.
[214] Z. Li, D. Guo, F. Li, G. Hou, X. Liu, C. Li, L. Cao, R. Wei, Z. Zhou, Z. Lai, Nerve network-inspired solid polymer electrolytes (NN-SPE) for fast and single-ion lithium conduction, Energy Storage Mater. 49 (2022) 575–582, https://doi.org/10.1016/j.ensm.2022.05.003.
[215] R.-A. Tong, H. Luo, L. Chen, J. Zhang, G. Shao, H. Wang, C.-A. Wang, Constructing the lithium polymeric salt interfacial phase in composite solid-state electrolytes for enhancing cycle performance of lithium metal batteries, Chem. Eng. J. 442 (2022) 136154, https://doi.org/10.1016/j.cej.2022.136154.
[216] M. Liu, X. Guan, H. Liu, X. Ma, Q. Wu, S. Ge, H. Zhang, J. Xu, Composite solid electrolytes containing single-ion lithium polymer grafted garnet for dendrite-free, long-life all-solid-state lithium metal batteries, Chem. Eng. J. 445 (2022) 136436, https://doi.org/10.1016/j.cej.2022.136436.
[217] J. Shen, Z. Lei, C. Wang, An ion conducting ZIF-8 coating protected PEO based polymer electrolyte for high voltage lithium metal batteries, Chem. Eng. J. 447 (2022) 137503, https://doi.org/10.1016/j.cej.2022.137503.
[218] K. Pan, L. Zhang, W. Qian, X. Wu, K. Dong, H. Zhang, S. Zhang, A flexible ceramic/polymer hybrid solid electrolyte for solid-state lithium metal batteries, Adv. Mater. 32 (2020) 2000399, https://doi.org/10.1002/adma.202000399.
[219] A. Kondori, M. Esmaeilirad, A.M. Harzandi, R. Amine, M.T. Saray, L. Yu, T. Liu, J. Wen, N. Shan, H.-H. Wang, A.T. Ngo, P.C. Redfern, C.S. Johnson, K. Amine, R. Shahbazian-Yassar, L.A. Curtiss, M. Asadi, A room temperature rechargeable Li_2O-based lithium-air battery enabled by a solid electrolyte, Science 379 (2023) 499–505, https://doi.org/10.1126/science.abq1347.
[220] X. Yi, Y. Guo, S. Chi, S. Pan, C. Geng, M. Li, Z. Li, W. Lv, S. Wu, Q. Yang, Surface Li_2CO_3 mediated phosphorization enables compatible interfaces of composite polymer electrolyte for solid-state lithium batteries, Adv. Funct. Mater. 33 (2023) 2303574, https://doi.org/10.1002/adfm.202303574.
[221] Y. He, Y. Qiao, Z. Chang, H. Zhou, The potential of electrolyte filled MOF membranes as ionic sieves in rechargeable batteries, Energy Environ. Sci. 12 (2019) 2327–2344, https://doi.org/10.1039/C8EE03651A.
[222] M. Cai, C. Zheng, J. Li, C. Shi, R. Yin, Z. Ren, J. Hu, Y. Li, C. He, Q. Zhang, X. Ren, Revealing the role of hydrogen bond coupling structure for enhanced performance of the solid-state electrolyte, J. Colloid Interface Sci. 652 (2023) 529–539, https://doi.org/10.1016/j.jcis.2023.08.046.
[223] M. Wu, S. Han, S. Liu, J. Zhao, W. Xie, Fire-safe polymer electrolyte strategies for lithium batteries, Energy Storage Mater. 66 (2024) 103174, https://doi.org/10.1016/j.ensm.2024.103174.
[224] L. Wu, F. Pei, D. Cheng, Y. Zhang, H. Cheng, K. Huang, L. Yuan, Z. Li, H. Xu, Y. Huang, Flame-retardant polyurethane-based solid-state polymer electrolytes enabled by covalent bonding for lithium metal batteries, Adv. Funct. Mater. (2023) 2310084, https://doi.org/10.1002/adfm.202310084.
[225] Q. Lv, Y. Song, B. Wang, S. Wang, B. Wu, Y. Jing, H. Ren, S. Yang, L. Wang, L. Xiao, D. Wang, H. Liu, S. Dou, Bifunctional flame retardant solid-state electrolyte toward safe Li metal batteries, J. Energy Chem. 81 (2023) 613–622, https://doi.org/10.1016/j.jechem.2023.02.040.
[226] X. Wang, D. Guan, C. Miao, J. Li, J. Li, X. Yuan, X. Ma, J. Xu, Boundary-free metal–organic framework glasses enable highly stable all-solid-state lithium–oxygen battery, Adv. Energy Mater. 14 (2024) 2303829, https://doi.org/10.1002/aenm.202303829.
[227] W.-X. Liu, X.-C. Huang, Y. Meng, D. Xiao, Y. Guo, A hybrid solid-state electrolyte endows a Li metal battery with excellent cycling life at 120 °C, J. Mater. Chem. A 11 (2023) 13446–13458, https://doi.org/10.1039/D3TA01588B.